

NPS ARCHIVE
1969
BEAM, J.

INVESTIGATIONS IN THE VACUUM ULTRAVIOLET
OF A STEADY STATE NITROGEN PLASMA

by

James Carlin Beam

United States Naval Postgraduate School



THESIS

INVESTIGATIONS IN THE VACUUM ULTRAVIOLET
OF A STEADY STATE NITROGEN PLASMA

by

James Carlin Beam

June 1969

T 132 485

This document has been approved for public release and sale; its distribution is unlimited.

Investigations in the Vacuum Ultraviolet
of a Steady State Nitrogen Plasma

by

James Carlin Beam
Lieutenant Commander, United States Navy
B.S., Naval Academy, 1960

Submitted in partial fulfillment for the
requirements for the degree of

MASTER OF SCIENCE IN PHYSICS

from the

work was partially supported by Naval Ordnance Laboratory,
Pak, under order number P.O. 7-0034.



Investigations in the Vacuum Ultraviolet
of a Steady State Nitrogen Plasma

by

James Carlin Beam
Lieutenant Commander, United States Navy
B.S., Naval Academy, 1960

Submitted in partial fulfillment for the
requirements for the degree of

MASTER OF SCIENCE IN PHYSICS

from the

NAVAL POSTGRADUATE SCHOOL
June 1969

ABSTRACT

In preparation for studies of shock waves in a collisionless plasma, a grazing incidence vacuum spectrograph has been used to study the vacuum ultraviolet spectra of a nitrogen plasma. The spectra are formed by a concave grating with a 1-meter radius of curvature and recorded on Kodak SWR (Shortwave-Radiation) Film. Analysis of the spectra was by comparison with helium and argon spectra, with intensity information from densitometric measurement using a Leeds and Northrup recording densitometer. Relative intensity determination provides an electron temperature evaluation technique.

Details on the modification of the Naval Postgraduate School plasma facility to accommodate a theta-pinch shock generation experiment are presented. Revised operating procedures for the new system configuration are included in the appendix.

A total of 735 lines was observed in the range 300-2000 angstroms. Relative intensity measurements indicated electron temperatures in the range 7.3 to 19.7 electron volts. Predicted relative intensities using a variable combination of the Local Thermal Equilibrium and Corona plasma models showed good sensitivity to temperature, but little difference between models.

TABLE OF CONTENTS

SECTION	PAGE
I. BACKGROUND AND THEORY -----	7
A. INTRODUCTION -----	7
B. GRAZING INCIDENCE SPECTROSCOPY -----	8
C. NITROGEN PLASMA -----	11
D. LTE AND CORONA PLASMA RADIATION MODELS -----	13
II. APPARATUS -----	18
A. SPECTROGRAPH -----	18
B. SPARK GAP CALIBRATION SOURCE -----	20
C. PLASMA SYSTEM -----	23
D. THETA-PINCH SHOCK GENERATION -----	29
III. EXPERIMENTAL TECHNIQUES -----	32
A. INSTALLATION OF GRATING -----	32
B. OPERATION OF VACUUM SPECTROGRAPH -----	34
C. SPECTRAL ANALYSIS -----	34
D. PLASMA SYSTEM OPERATION -----	37
E. THETA-PINCH SHOCK WAVE STUDY -----	38
IV. OBSERVATIONS AND RESULTS -----	39
A. NITROGEN PLASMA SPECTRUM -----	39
B. RELATIVE LINE INTENSITIES -----	39
C. ELECTRON TEMPERATURE EVALUATION -----	42
D. THETA-PINCH PERTURBATION -----	43
V. CONCLUSIONS AND RECOMMENDATIONS -----	45
A. SPECTROGRAPHIC ANALYSIS -----	45
B. TIME RESOLVED PHOTOMETRY -----	46

C. VUV SCANNING MONOCHROMATOR -----	46
D. MAGNETIC FIELD SURVEY -----	47
E. SPARK GAP SPECTRAL STUDIES -----	47
APPENDIX A - PLASMA SYSTEM OPERATING PROCEDURE -----	48
APPENDIX B - VUV SPECTROGRAPH OPERATION -----	55
APPENDIX C - NITROGEN-HELIUM SPECTRUM -----	57
APPENDIX D - NITROGEN SPECTRUM -----	66
APPENDIX E - NITROGEN GROTRIAN DIAGRAMS -----	67
APPENDIX F - ELECTRON TEMPERATURE PROGRAM -----	71
APPENDIX G - RELATIVE LINE INTENSITY PROGRAM -----	77
BIBLIOGRAPHY -----	80
INITIAL DISTRIBUTION LIST -----	82
FORM DD 1473 -----	83

LIST OF ILLUSTRATIONS

FIGURE	PAGE
1. Grazing Incidence Spectrograph Optics -----	10
2. Vacuum Ultraviolet Spectrograph Operational Schematic -----	19
3. Spark Gap Ionization Source Circuit Schematic -----	21
4. Spark Ionization Spectra, Electrode Design -----	22
5. Plasma System OLD Configuration -----	24
6. Plasma Vacuum Control Schematic -----	26
7. Plasma System NEW Configuration -----	27
8. Cathode - Anode Section -----	28
9. Theta - Pinch Circuit Schematic -----	30
10. Theta - Pinch Coil -----	31
11. VUV Spectrograph Focus - O ₂ Absorption Lines -----	33
12. Nitrogen-Helium Spectrum -----	65
13. Nitrogen Spectrum -----	66
14. Argon Spectra -----	36

ACKNOWLEDGEMENTS

It is not possible to personally thank the many persons who contributed to this project. The author wishes to sincerely thank Professors Alfred W. Cooper, Sydney H. Kalmbach, and Raymond L. Kelly for their support and guidance throughout the work. The author is also indebted to Miss Sarah Jaite and Mr. William C. Butzlaff for their computer programming assistance, to Mr. Hal Herreman for technical advice and supervision, and to Mr. Michael O'Dea and Mr. Peter Wisler of the Naval Postgraduate School Machine Shop Facility for their component fabrication and technical support. This work was partially supported by U. S. Naval Ordnance Laboratory, White Oak, Maryland.

I. BACKGROUND AND THEORY

A. INTRODUCTION

Modification of the Naval Postgraduate School reflex arc plasma facility to accommodate a shock wave generation experiment has been completed. The disturbance in the plasma column is accomplished by a short period capacitor discharge through a single coil mounted coaxially with the plasma vacuum tube. Investigation of the shock wave generation, velocity, and attenuation in a nitrogen plasma is presently being conducted. Background investigations of the visible and ultraviolet radiation emitted by the steady state plasma were necessary prior to the investigation of shock front emissions. The object of this investigation was to provide a spectral survey of the nitrogen plasma in the vacuum ultraviolet region under varying conditions of longitudinal magnetic field strength and at different locations along the ten foot plasma column. Some work was also completed in evaluating electron temperatures from observed spectral line relative intensities.

The entire shock disturbance program was undertaken in an attempt to solve investigative problems in studies of shock waves in low pressure atmospheric gases. Previous experimentation has been hampered by impurity problems and by atmospheric absorption of emitted radiation. The solution to these problems could best be accomplished through study of a magnetically confined laboratory plasma. Use of vacuum ultraviolet detectors is of considerable importance in radiation studies of multiple-ionized gases, since the most intense emission lines occur in the vacuum ultraviolet.

This report describes the vacuum ultraviolet investigation of the nitrogen plasma, modification of the plasma system for shock wave studies, and presents identifications of the observed spectra. Additionally, two computer programs are presented for use in spectral analysis. One is a more sophisticated version of previous work in electron temperature evaluation from relative line intensities based on either local thermal equilibrium or corona conditions. The second generates predicted relative intensities for fixed electron temperatures based on various combinations of LTE and corona radiation models.

Past work in the steady state nitrogen plasma includes probe measurements of electron temperatures [1], a spectral survey of the visible nitrogen spectrum, and preliminary intensity analysis using a dual beam spectrophotometer [2]. Investigations continue in both areas. Previous vacuum ultraviolet investigation was limited to argon and helium plasmas [3].

B. GRAZING INCIDENCE ULTRAVIOLET SPECTROSCOPY

Investigations in the region above 1000 \AA may be made with conventional mountings of diffraction gratings at normal incidence. Reflectance of concave gratings, although of low magnitude in the range 1000 \AA to 2000 \AA , is acceptable provided a suitable vacuum-deposited reflecting film is used. The material most generally used is platinum, which for normal incidence has a reflectance of 22% for radiation as short as 600 \AA [4]. For investigations of wavelengths below 600 \AA one must resort to grazing incidence spectroscopy. As suggested by past research in the vacuum ultraviolet, a one-meter radius of curvature concave grating has been platinum coated for use

at grazing incidence. There are no suitable transmittance optics in this region. Even the number of reflections must be kept to an absolute minimum. For these reasons, the vacuum ultraviolet spectrograph was designed to utilize a Rowland mounted concave grating at grazing incidence.

The spectrograph optics are shown schematically in Fig. 1. Angle of incidence is set at 82° . The theory of operation of the concave grating has been discussed in detail by Beutler [5] and others. The fact that Rowland conditions are valid at grazing incidence allows rather simple evaluation of the reciprocal dispersion as:

$$\frac{d\lambda}{d\ell} = \frac{d}{m R} \cos \psi$$

where ℓ is the distance from the central image to the position of a spectral line of wavelength λ (as measured along the Rowland circle), d/m is the groove spacing of the grating, and ψ is the angle of diffraction. The reciprocal dispersion of the grating used is summarized below.

ψ	$d\lambda/d\ell$
0°	$16.7 \frac{\text{\AA}}{\text{mm}}$
45°	11.8
75°	4.32
80°	2.90
81°	2.61
82°	2.33
83°	2.04

Note from the equation that $d\ell/d\lambda$ is directly proportional to $1/\cos \psi$. Thus as ψ approaches 90° , $d\ell/d\lambda$ becomes infinite.

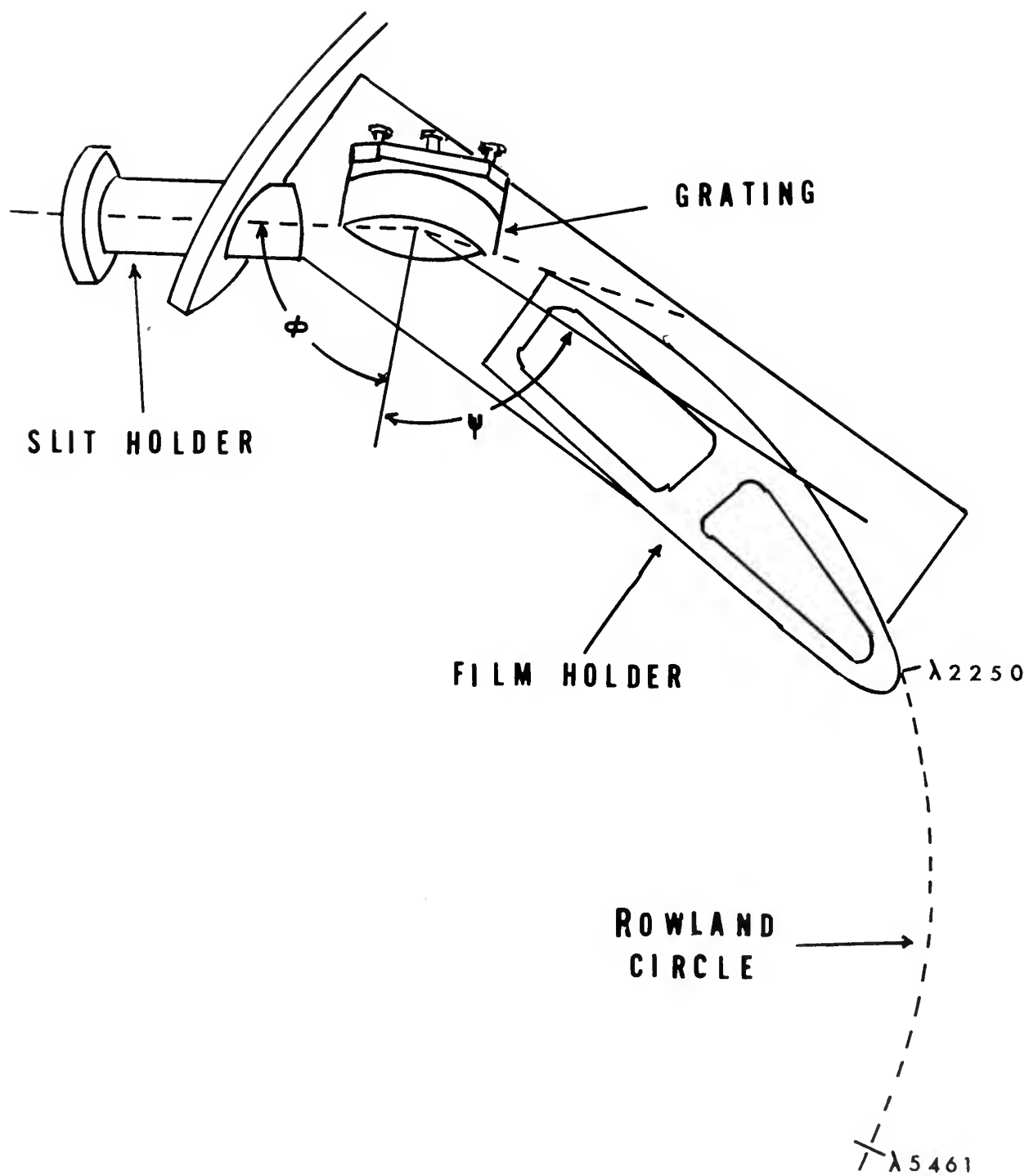


FIG. 1
GRAZING INCIDENCE
SPECTROGRAPH OPTICS

The advantage of higher angular dispersion at grazing incidence is obvious. Resolving power, on the other hand, decreases at grazing incidence. As shown by Samson [6], resolving power is directly proportional to the optimum width of the grazing which decreases from 21.6 cm at normal incidence to 2.2 cm at 80° incidence for a wavelength of 500 \AA .

C. NITROGEN PLASMA

Previous studies have described the steady state reflex arc. Ionization has been estimated at 95%. Electron temperatures on the order of 4.0 eV have been reported by Orlicki [7], et al, although a computer program error affected the results slightly. Present work with Langmuir probes and a dual beam spectrophotometer indicates values of electron temperatures in the range 3.5 to 8.0 eV. Previous estimates of ion temperatures are $5 \times 10^3 \text{ }^\circ\text{K}$ maximum, and electron densities approximately $2 \times 10^{18}/\text{m}^3$. The ion temperature was estimated from previous unpublished work on interferometer measurement of Doppler broadening. Null results make the assumed value an upper limit of the ion temperature.

Of particular importance in considering possible diagnostics for shock wave investigation are the characteristic collision times. Relative line intensity analysis is dependent on the assumed radiation model. Determination of the time required for a perturbed plasma to restore itself to the condition of local thermal equilibrium is necessary to establish the validity of using an LTE based intensity analysis. Based on electron-ion collision time equations developed by Spitzer [8], and Rose and Clark [15]

$$\left. \begin{array}{l} \tau_{\theta ee} \\ \tau_{\theta ii} \end{array} \right\} = \frac{25.8 \sqrt{\pi} \epsilon_0^2 m^{1/2} (kT)^{3/2}}{q^4 n_{e,i} \ln \Lambda}$$

where Λ is a measure of the number of electrons in a Debye sphere and other symbols are well known. For electron-ion and ion-electron collisions the collision times are given by

$$\frac{m_e}{m_i} \tau_{\theta ie} = \tau_{\theta ei} = \frac{32 \sqrt{2\pi} \epsilon_0^2 m_e^{1/2} (kT_e)^{3/2}}{(Zq^2)^2 n_i \ln \Lambda}$$

Assuming for the NPGS plasma the following parameters according to previous evaluations;

$$T_e = 5 \times 10^4 \text{ } ^\circ\text{K}$$

$$T_i = 5 \times 10^3 \text{ } ^\circ\text{K}$$

$$n_e = n_i = 2 \times 10^{18} / \text{m}^3$$

$$\ln \Lambda = 10 \text{ (as given by Spitzer)}$$

we find for the collision times:

$$\tau_{\theta ee} = 0.148 \times 10^{-6} \text{ sec}$$

$$\tau_{\theta ii} = 0.754 \times 10^{-6} \text{ sec } (N^+)$$

$$\tau_{\theta ei} = 260.8 \times 10^{-6} \text{ sec}$$

$$\tau_{\theta ie} = 6.7 \text{ sec } (N^+)$$

Since scattering of ions by electrons is much slower than relaxation through ion-ion collisions, it is expected that any effects of a disturbance which selectively heats ions may be observed as increased ion temperature and that analysis may assume equilibrium conditions.

In particular, for a shock front which raises the ion temperature to just double the electron temperature, calculations assuming the previous electron temperature give an ion-ion collision time of 67.5×10^{-6} sec for N^+ . In collisionless heating of the plasma most of the energy should be transferred to the ions, making the previous assumptions plausible. It may be concluded that shock perturbation of the ion temperature will be observable, but time resolution may be necessary.

D. LTE AND CORONA PLASMA RADIATION MODELS

Quantitative spectral analysis requires the assumption of specific equilibrium conditions in the plasma. The simplest of the radiation models is the assumption of local thermal equilibrium. LTE as defined by McWhirter [9] assumes that the distribution of electron density populations is determined by particle collision processes with immediate response to changes in plasma conditions. Electron collision processes dominate with electrons having a Maxwellian distribution. Observation of a particular area of the plasma gives average values of electron temperature and density over the area. The plasma parameters may have time and spatial variation, but population densities for any point are uniquely determined by the local values of temperature, density, and composition. Relative number densities of like species may be expressed solely in terms of the appropriate statistical weights and Boltzmann factors; e.g.,

$$N_n/N_m = \frac{g_n \exp(-E_n/kT)}{g_m \exp(-E_m/kT)}$$

Local thermal equilibrium requires negligible radiative decay. This condition is met most closely in dense laboratory plasmas. When the

plasma electron density decreases to the point where radiative decay becomes important LTE is no longer a valid model.

Based on the probability of radiative transitions being comparable with collisional transitions under certain conditions, McWhirter has derived a validity criterion for the assumption of local thermal equilibrium. The criterion,

$$n_e \geq 1.6 \times 10^{12} T_e^{1/2} \chi(p,q)^3 \text{ cm}^{-3}$$

where,

n_e = electron density (cm^{-3})

T_e = electron temperature ($^{\circ}\text{K}$)

$\chi(p,q)$ = excitation potential of level p from level q (volts)

Using the previously stated average electron temperature of $5 \times 10^4 \text{ }^{\circ}\text{K}$, $\chi(p,q) = 11\text{v}$ (for the 1200 \AA transition of NI), then the electron density must be greater than $4.76 \times 10^{17} \text{ cm}^{-3}$. Previously estimated electron densities are nowhere near this magnitude. Griem [10] has suggested that the validity criterion may be even more stringent since actual plasmas are both inhomogeneous and time dependent. On the other hand, if quantitative results from assumption of local thermal equilibrium agree with independent diagnostic methods, LTE may give acceptable results for certain ion species. The simplicity of the LTE model makes its use desirable whenever possible.

At the other extreme is the assumption that collisional ionization and excitation are balanced by radiative recombination and spontaneous decay. This model is the corona-radiative plasma model described in detail by Griem [10], McWhirter [9], and others. Population density distributions are now based on the assumption of a Maxwellian velocity distribution for free electrons as in the LTE model and balance between

collisional excitation from the ground level and spontaneous radiative decay instead of the collisional balance of LTE. This balance condition is met in cases where the electron density is too low to meet the validity criterion for LTE.

Line intensities are dependent on the relative number of electrons in an excited state, probability for the particular transition from that state to occur, and observational probability with respect to the emitted radiation. Population densities are determined by excitation and de-excitation processes in the plasma. Atomic transition probabilities prescribe the most likely route for de-excitation of an excited state. Observational probability is disregarded by assumption that the plasma is optically thin; i.e., emitted radiation is not self-absorbed by the plasma. A very general expression for spectral line intensity is then,

$$I(p,q) = 1/4\pi \int n(p) A(p,q) h\nu(p,q) ds$$

where $n(p)$ is the population density of level p , $\nu(p,q)$ is the frequency of the emitted photon, and $A(p,q)$ is the atomic transition probability for the transition between bound levels p and q . $A(p,q)$ may be evaluated quantum mechanically using various theoretical approximations (notably the Coulomb approximation and Self-Consistent Field approximation) or experimentally from the previous equation.

If intensities are to be used in plasma electron temperature analysis, the line intensity ratio technique is most generally used. This avoids the requirements for absolute intensity measurements and determination of population density distributions when the observed spectral lines are of the same species.

Assuming local thermal equilibrium, electron temperatures may be evaluated through knowledge of relative spectral line intensities by using an equation given by Robinson and Lenn [11]:

$$T_e = \frac{E_{m2} - E_{m1}}{k \ln \left[\frac{I_1}{I_2} \frac{g_2}{g_1} \frac{f_2}{f_1} \left(\frac{\lambda_1}{\lambda_2} \right)^3 \right]}$$

where, E_{m1}, E_{m2} = excitation energies of the first and second levels, respectively

k = Boltzmann constant

I_1, I_2 = relative line intensities

g_1, g_2 = statistical weights of the upper states

f_1, f_2 = absorption oscillator strengths

λ_1, λ_2 = wavelengths of the transitions

This equation may be developed from the expression for the absolute line intensity,

$$I_{mn} = [A_{mn} (E_m - E_n) g_m N/Q] \exp (-E_m/kT_e)$$

where N is the species number density, Q is the internal partition function, and other terms are as previously defined. Again it is seen that line intensities are dependent on the population distribution of electrons in the excited state, $N \exp (-E_m/kT_e)$, and the probability of the transition A_{mn} . Dividing the above expression by a like equation for another transition of the same atomic species, number densities and the internal partition functions are eliminated.

$$\frac{I_1}{I_2} = \frac{g_1 A_{11} \nu_1}{g_2 A_{22} \nu_2} \exp [-(E_{m1} - E_{m2})/kT_e]$$

Additionally, intensities need not be measured absolutely since on solving for T_e , the intensities appear as a ratio. Only the relative strengths are necessary. Using the expression for atomic transition probability in terms of the absorption oscillator strength, f_{mn} ,

$$A_{mn} = \text{constant} \times f_{mn} / \lambda^2$$

the expression given for electron temperature is reached.

The Corona model is very similar in terms of analysis to the LTE model. Balance of the collisional-excitation rate from the ground state with the spontaneous decay rate brings in a factor of $(E_{m1}/E_{m2})^3$ in the expression for the number density. This modification of the Saha-Boltzmann equations does not cancel for line ratio expressions since the excitation potentials of the two excited levels are usually not the same. Based on this departure from the Boltzmann and Saha equations for distributions of population densities, the electron temperature as given for Local Thermal Equilibrium is changed to:

$$T_e = \frac{E_{m2} - E_{m1}}{k \ln \left[\frac{\frac{I_1}{I_2} \frac{g_2}{g_1} \frac{f_2}{f_1} \left(\frac{E_1}{E_2} \right)^3 \left(\frac{\lambda_1}{\lambda_2} \right)^3}{1} \right]}$$

where all symbols are previously defined. A computer program is given in Appendix F to derive electron temperatures for either model. The computer program given in Appendix G will generate relative line intensities from known electron temperatures and mixes of the two basic radiation models. Values for oscillator strengths and statistical weights were obtained from Griem [10] and Wiese, Smith, and Glennon [12].

II. APPARATUS

A. SPECTROGRAPH

The grazing incidence vacuum spectrograph used for the vacuum ultraviolet survey of the nitrogen plasma was designed by R. L. Kelly [13]. It has survey capability in the range 100 - 2250 Å and is compatible with the NPGS plasma reflex arc vacuum system. A schematic diagram shows the principal features of the spectrograph (Fig. 1). Mounted on the front plate of the vacuum tank is a slit assembly with entrance slit set at 15 microns. The grating mount and film holder are supported by a channel beam welded to the front plate. The vacuum enclosure consists of a 10-inch I.D. aluminum tube which bolts to the front plate. The rear of the system has a removable back plate allowing film loading.

The grating used was a Bausch and Lomb replica diffraction grating with a 998.8 mm radius of curvature, 600 grooves per mm, blaze angle of $4^{\circ} 45'$ for a blaze wavelength of 2760 Å, used at 82° angle of incidence. This grating differed from the grating previously used in that it was platinum coated for greater reflectance in the extreme vacuum ultraviolet.

The spectrograph vacuum system consists of a 4" National Research Corporation Model 0161 diffusion pump and a Welch Scientific high vacuum Duo-Seal Model 1402 mechanical pump. In operation the combined pumping system provided, with cold trapping, a fifteen minute recycle capability from atmospheric pressure to one micron or less. The complete spectrograph system is shown in Fig. 2.

VACUUM ULTRAVIOLET SPECTROGRAPH OPERATIONAL SCHEMATIC

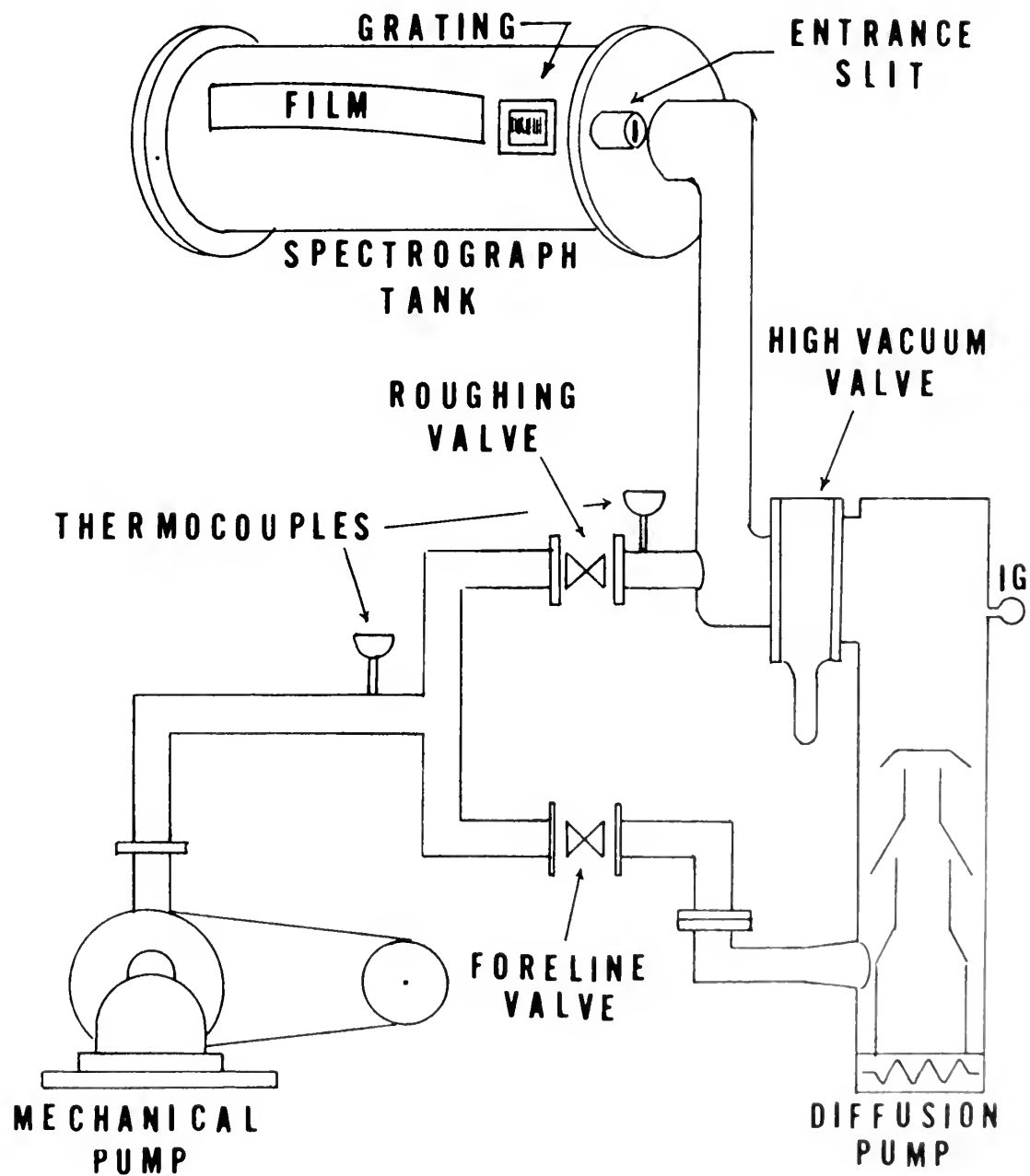
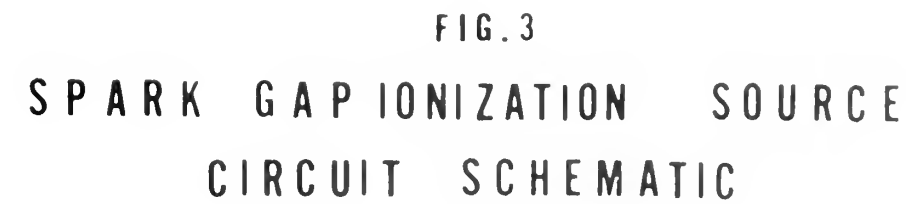


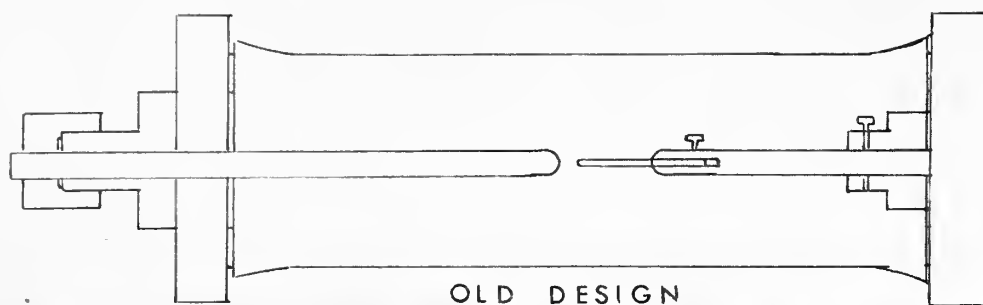
FIG. 2

No purging gas was used although there is a capability for purging through a variable leak connected to the vacuum tank vent. The variable leak was utilized in spark source focusing runs to optimize pressures for operation of the vacuum spark gap.

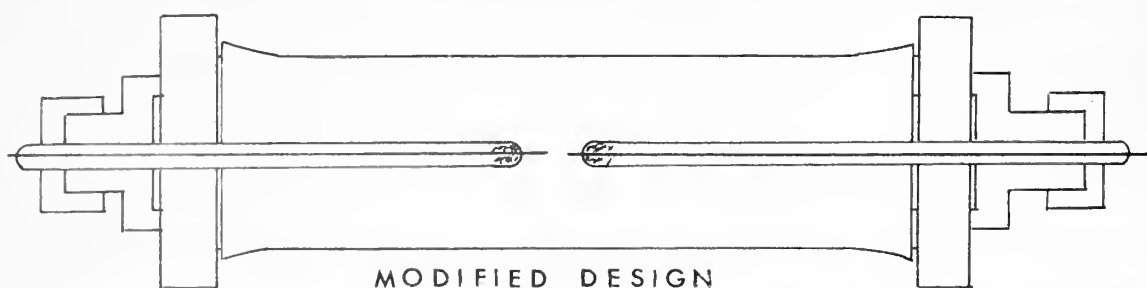
B. SPARK GAP CALIBRATION SOURCE

Positioning and focusing of the new platinum coated grating was accomplished in part through the use of a vacuum spark gap. The apparatus is described in detail by L. E. Kaufman [14]. The trigger circuit was by-passed to produce a free running spark with discharge potential controlled by the spacing of the trigger electrodes (spark gap switch). The circuit schematic (Fig. 3) shows the spark gap system as used. During initial calibration runs it was found that significant losses were developing in the coaxial cable from the air gap switch to the vacuum spark, in corona discharge at the electrode holder, and in secondary discharge between the aluminum end plates of the glass T pipe and the electrodes or between the thinly coated wall of the glass T pipe and the electrodes. The problem was solved by substitution of high voltage coaxial cable and by redesign of the electrode assembly. All possible corona points were eliminated and secondary discharge prevented by use of heavy gauge wire electrodes mounted in glass feed-throughs. The improvement in concentration of the discharge between the electrode pins was significant as shown by comparison spectra in Fig. 4. The number of sparks required to produce equivalent exposures was reduced by a factor of ten.





TUNGSTEN · ALUMINUM



TUNGSTEN · TUNGSTEN

FIG. 4
SPARK IONIZATION SPECTRA
ELECTRODE DESIGN

C. PLASMA SYSTEM

Initial survey of the nitrogen plasma was conducted with the plasma system configuration shown in Fig. 5. The nitrogen spectrum was scanned at each of the five access ports indicated in the figure. The discharge was operated with a hollow tantalum cathode at ground with respect to the fixed anode held at approximately 100 volts. Arc current was maintained at 60 amps although operation was possible over the range 40 to 120 amps for most conditions of magnetic field and gas supply pressure. At lower currents the discharge could not be maintained. Power requirements and cathode lifetimes set the upper limit. Main magnetic field current was set at 400 amps for the initial runs giving a field of approximately 2400 gauss at the center of the plasma column, as measured with a Hall probe. The field was uniform to within 15% between observation ports #1 and #5. Capability for variation of the magnetic field strength is from approximately 1200 gauss to 10,000 gauss. Neutral gas pressures were measured by an ion gauge positioned above port #3 and varied with the gas supply pressure from 8×10^{-5} mm Hg to 8×10^{-4} mm Hg. Oscillations of the plasma, which persisted for as much as two hours, occurred when the argon starting gas was replaced by nitrogen.

In order to accommodate a theta pinch-generated shock wave experiment the system was altered by insertion of a glass tube with 2 inch I.D. in place of Port #4. A straight section of 4 inch pyrex tube was placed between Port #3 and the anode chamber for use in a longitudinal wave study. Diffusion pump #1 was completely bypassed. The anode-cathode section was redesigned with the anode chamber positioned above a Clark 10" diffusion pump. A large manual gate valve separates the exhaust side of the 10" diffusion pump from the booster manifold,

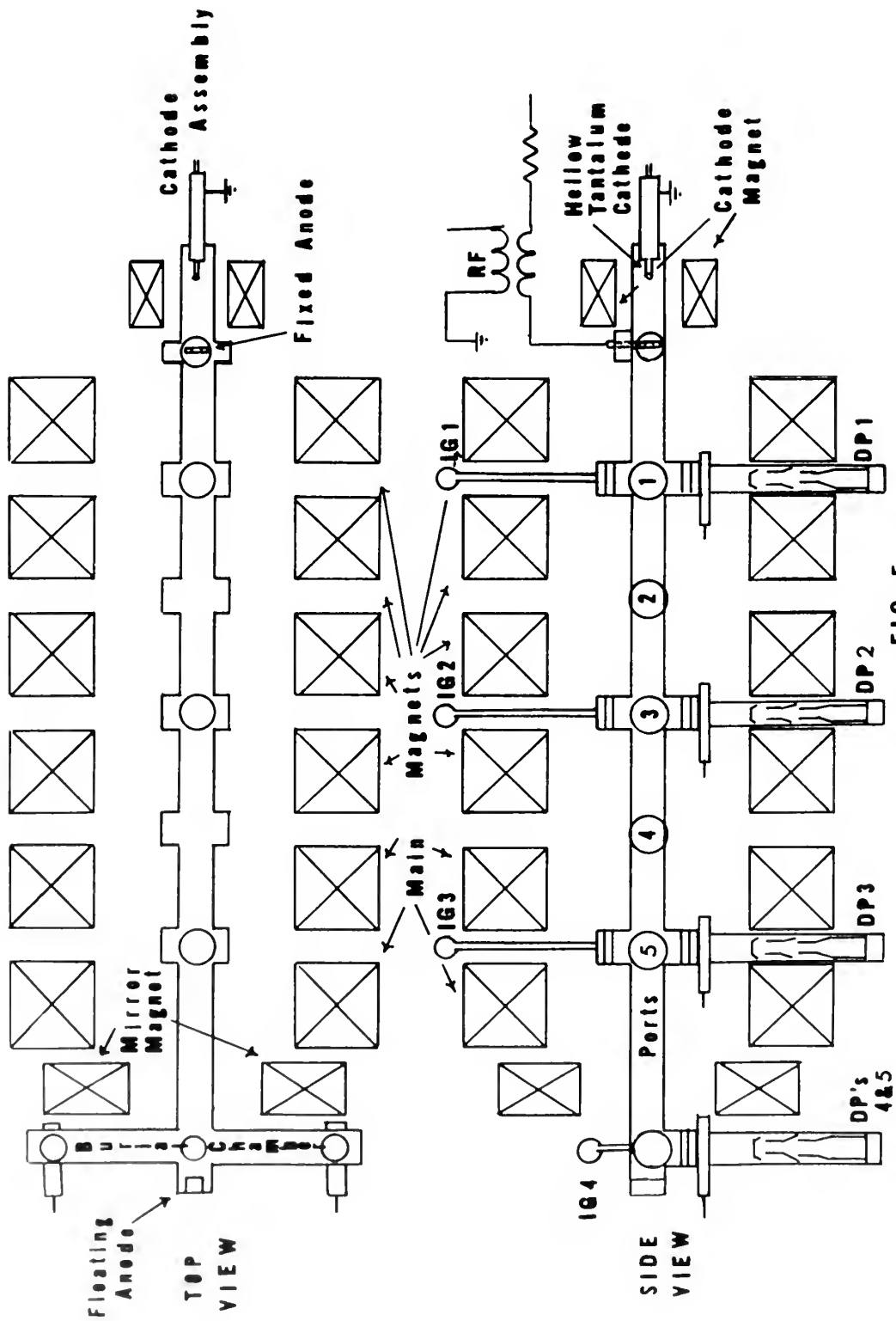


FIG. 5

PLASMA SYSTEM - OLD CONFIGURATION

but there is currently no provision for automatic valving between the diffusion pump and the vacuum chamber. This major alteration of the plasma vacuum system made it necessary to develop a set of standardized operating procedures to prevent damage to the diffusion pumps and the vacuum chamber. The vacuum control panel was redesigned as shown in Fig. 6. Operating procedures are presented in Appendix A. A schematic of the new vacuum system configuration is shown in Fig. 7. Details of the anode-cathode section are shown in Fig. 8. As depicted, five new magnets were wound from 1/4 inch square copper tubing for use on both ends of the cathode and anode chambers. When used with the designed number of water paths, each coil is capable of use at 300 amps/40 volts. At present, the number of water paths is reduced, setting a 150 amp current limit.

With the new configuration the system was operated with magnetic field strength varied from approximately 2400 to 6000 gauss. The mirror rectifier was reconnected to the mirror magnet for improvement of plasma confinement. Visible intensities improved slightly and the mirror magnet was set at 1000 amps for a field strength in the vicinity of the floating anode of 5600 gauss.

With the new configuration no instability problems developed on switching from argon to nitrogen, although the nitrogen plasma column was more diffuse than with the previous vacuum system. The previous instabilities appeared to be pressure related although no ranging of the operating parameters affected the instabilities. A possible explanation of the problem was insufficient gas throughput with the old system. The greater pumping capacity has made it necessary to operate with gas supply needle valves wide open and booster manifold pressures three times the previous values.

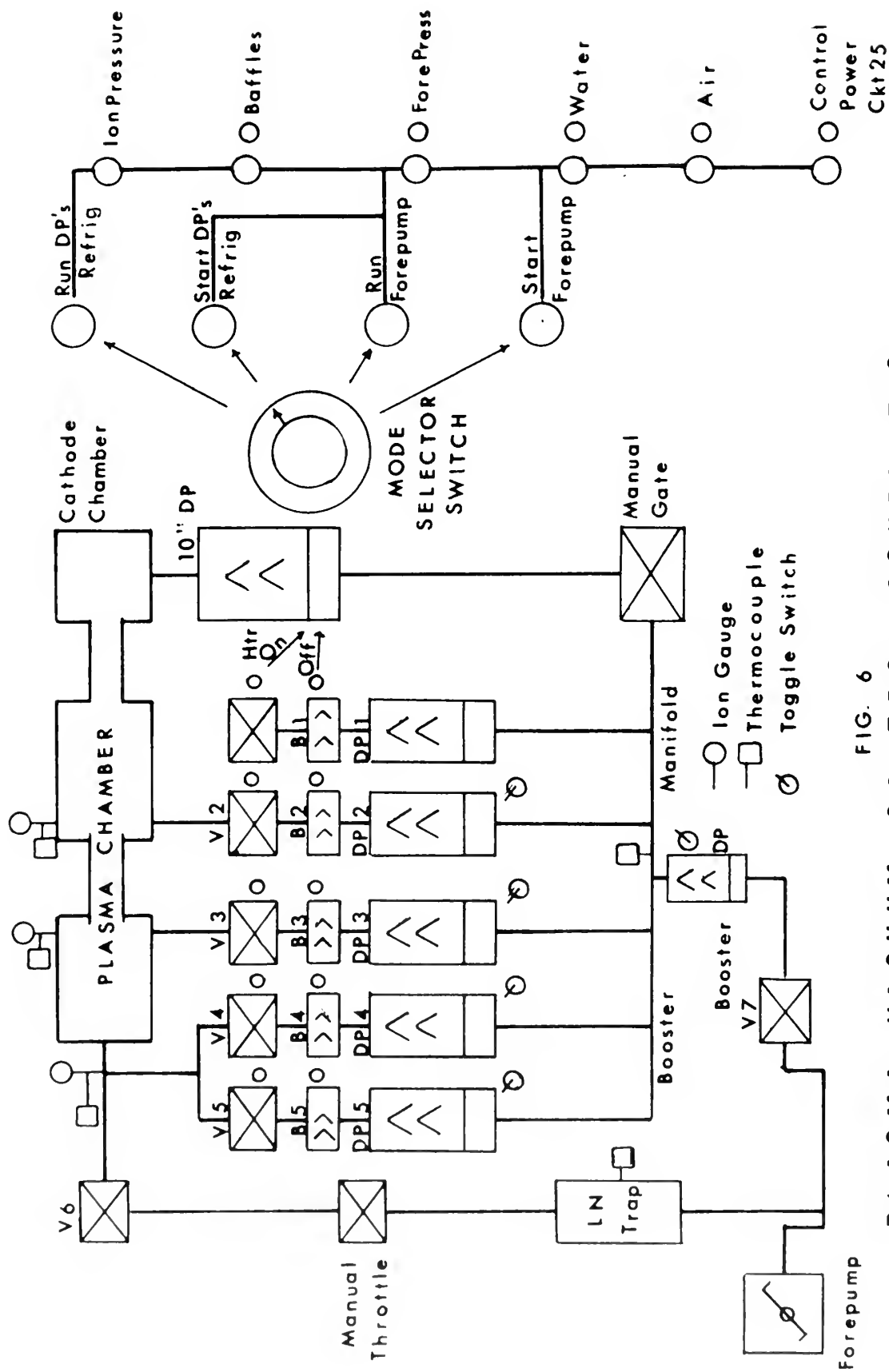


FIG. 6
PLASMA VACUUM CONTROL SCHEMATIC

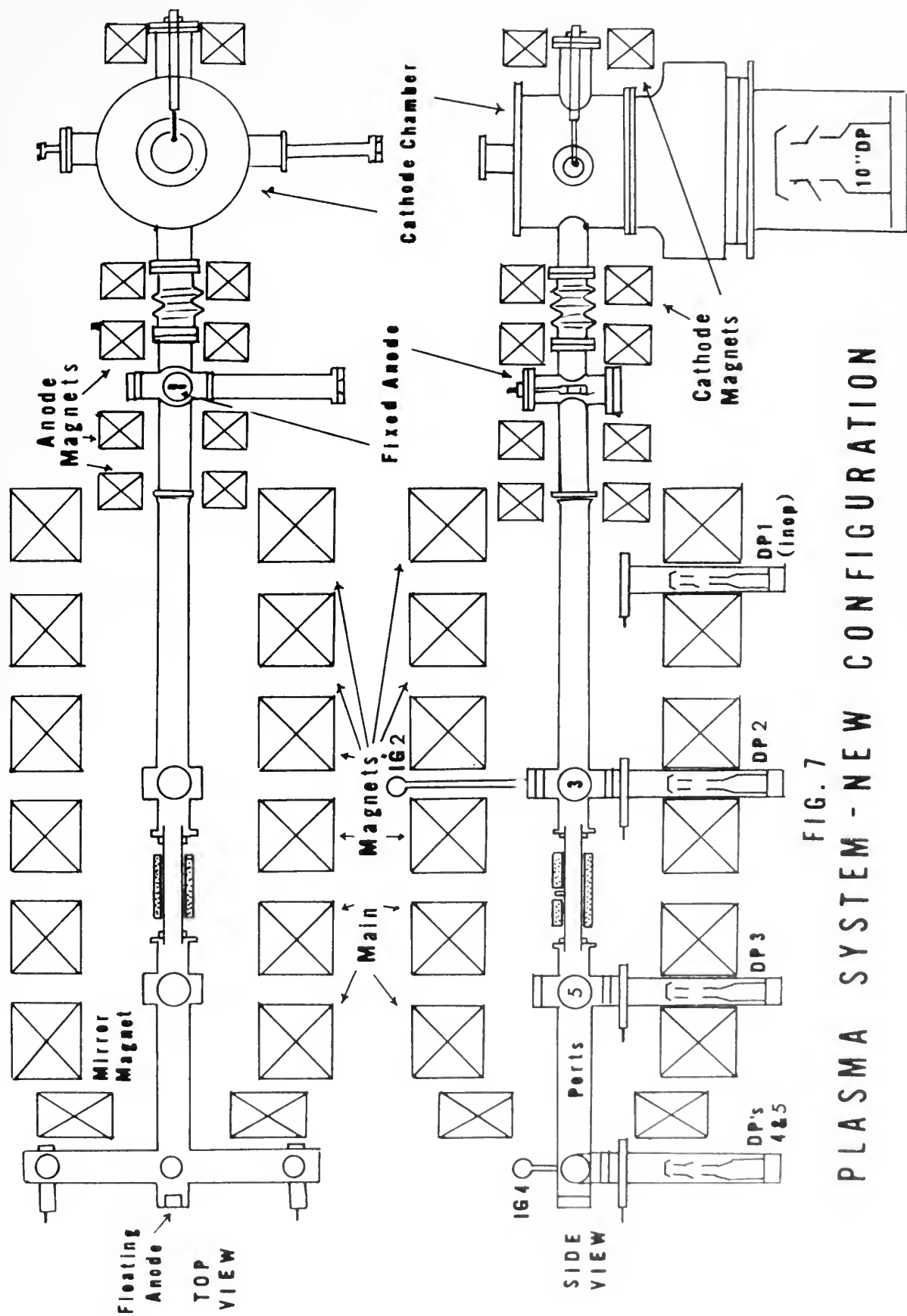


FIG. 7
PLASMA SYSTEM - NEW CONFIGURATION

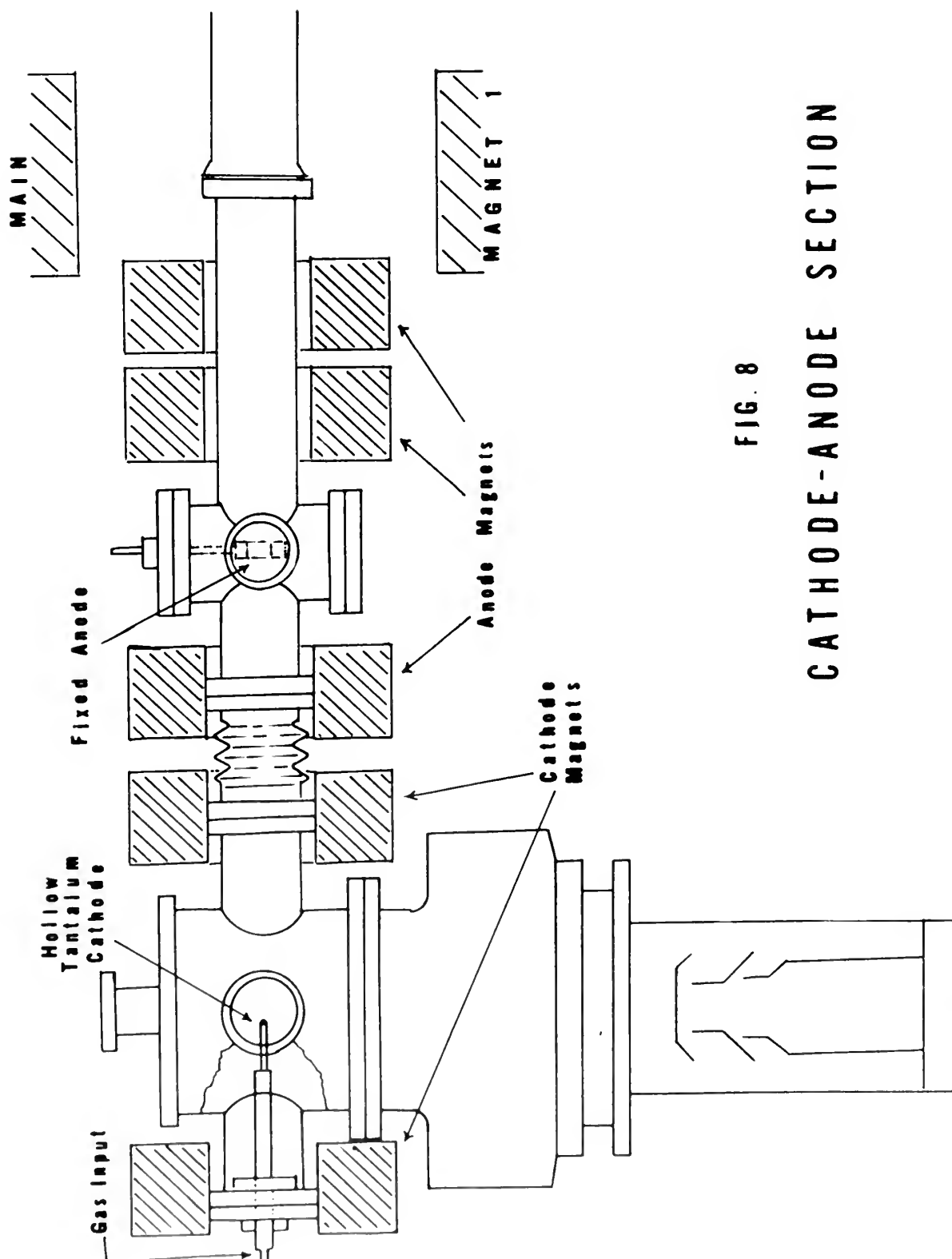


FIG. 8
CATHODE-ANODE SECTION

D. THETA PINCH SHOCK GENERATION

Installation of the theta pinch device was completed in May 1969. The system is sketched in Figs. 9, 10. At present the system is capable of discharging a 4.8×10^4 amp, 20 kilovolt pulse with a ringing frequency of approximately 1 megacycle. The pulse is discharged around a single turn coil that is coaxial with the plasma column. The concept of shock generation in this manner is similar to that used in the Scylla device as described by Rose and Clark [15]. Theory of operation of the theta-pinch is best described by Glasstone and Lovberg [16]. Discharge through the coil induces an oppositely directed azimuthal current which with the axial magnetic field causes a compressive force to act on the plasma column. Heating by magnetic compression shows great promise in thermonuclear work although significant problems in confinement develop. The purpose of the theta-pinch device in the NPGS plasma system however is to provide a fast compression generated shock wave in conditions qualitatively similar to the ionosphere.

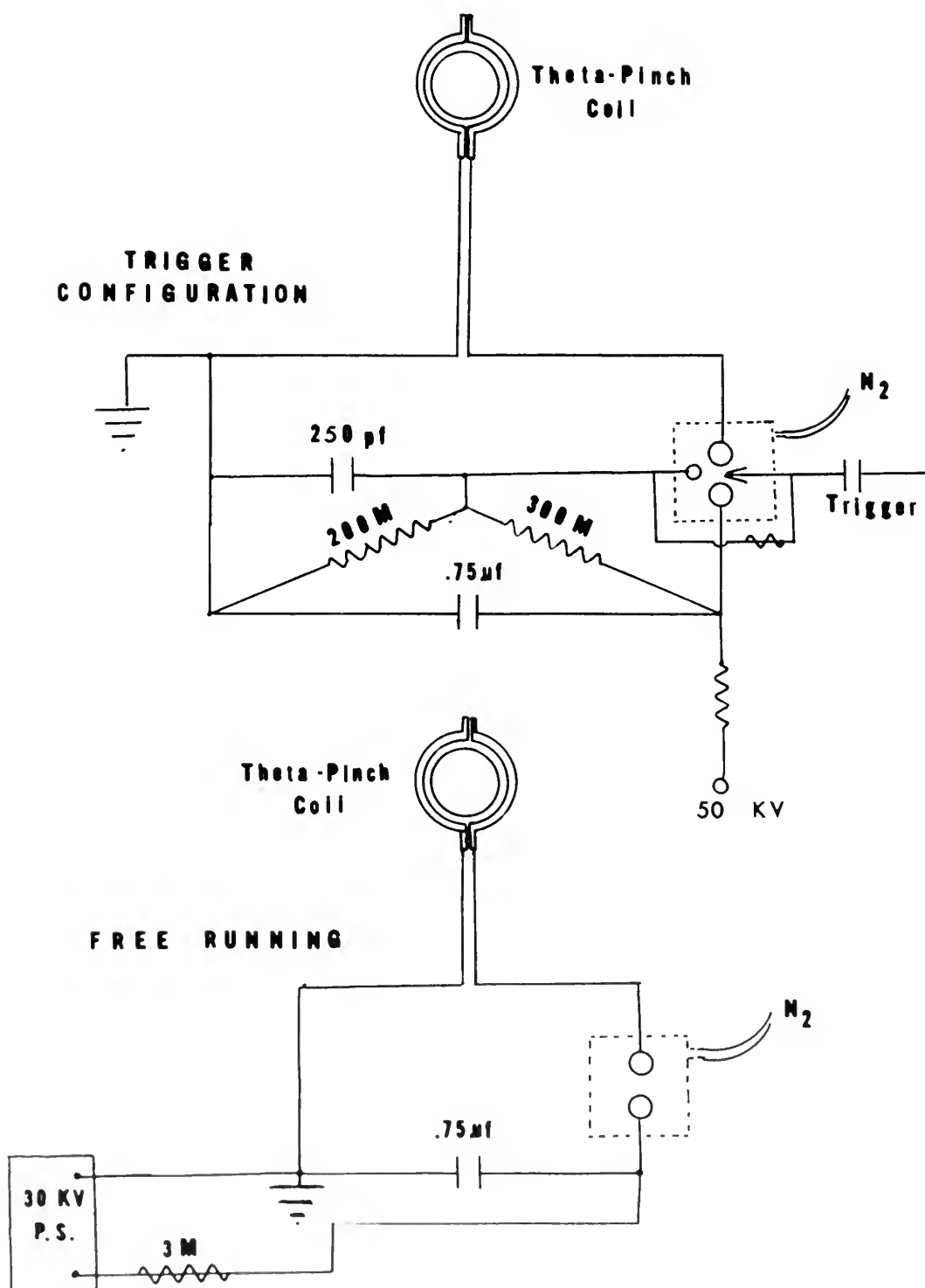


FIG. 9
THETA-PINCH CIRCUIT SCHEMATIC

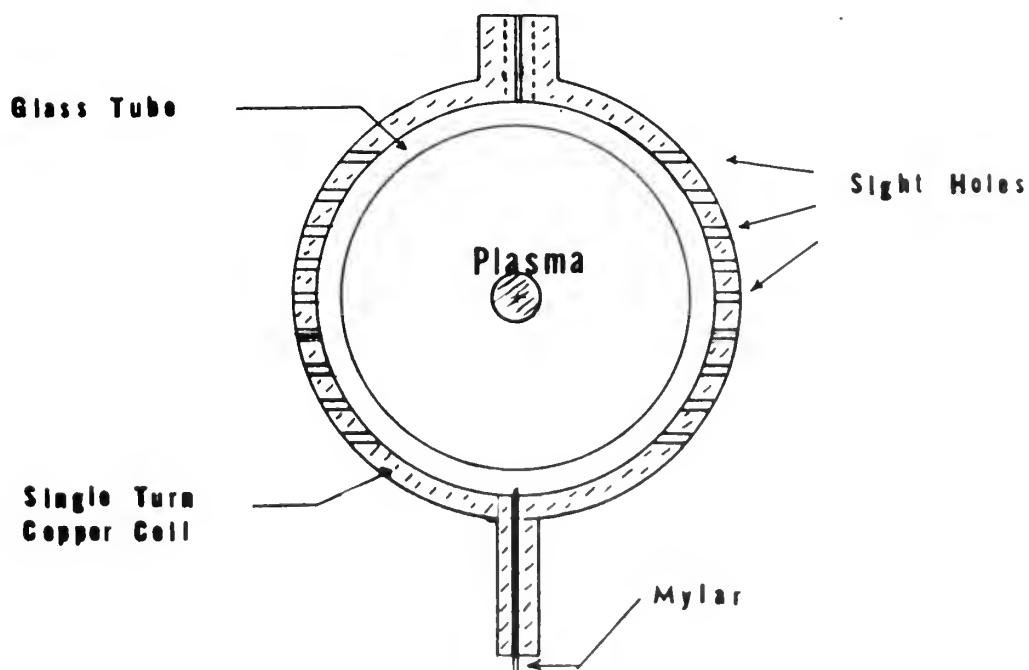
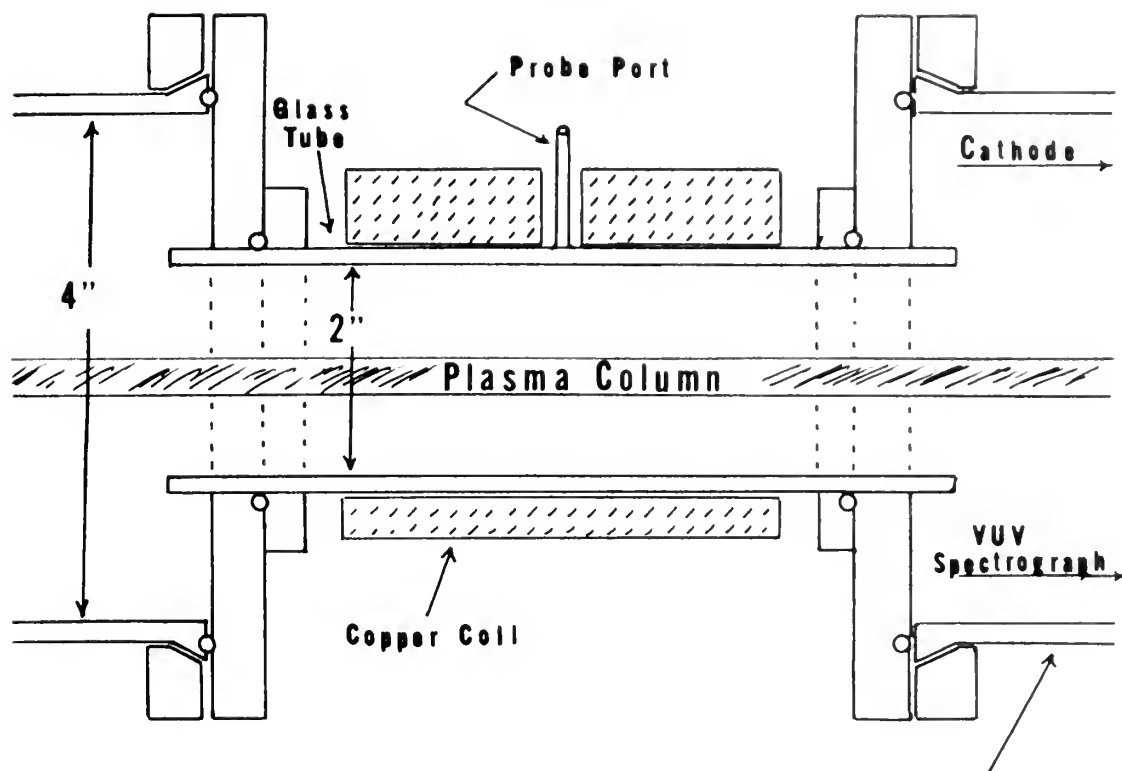


FIG. 10

THETA-PINCH COIL

III. EXPERIMENTAL TECHNIQUES

A. INSTALLATION OF GRATING

To improve the operating characteristics of the vacuum ultra-violet spectrograph, i.e., to reduce required exposure times, the previously used uncoated grating was replaced with a platinum coated grating with other characteristics identical. This was accomplished by establishing bench marks while the old grating was in place, then matching the new grating to these conditions. Fine focusing was accomplished using the continuous spectrum of a medium pressure mercury source and adjusting the grating for maximum sharpness of the O_2 absorption lines (Fig. 11). Overall focus was then checked in vacuum utilizing a tungsten-aluminum spark source. It became apparent after moving the spectrograph to the plasma source that substantial losses were occurring due to excessive downward rotation of the grating about a longitudinal axis. Observed spectral lines were extremely faint and extended over only a third of the film. The grating was then completely repositioned using a cathetometer in conjunction with a continuous beam laser to make coplanar the Rowland circle established by the grating and the plane established by the film holder. Extension of the Rowland circle permitted using the Hg green line as a focus check. Final focus was as above with the absorption spectrum and the tungsten-aluminum spectrum.

Major problems developed in the spark gap calibration source. Losses as described in the previous section in the coaxial cable and in stray discharge inside the glass T-tube reduced the efficiency of



VUV SPECTROGRAPH FOCUS
 O_2 ABSORPTION LINES



FIG. 11

the spark to the point where adequate calibration runs could not be made. Redesign of the electrodes and the power input system allowed exposures with ten or fewer sparks as compared to three hundred sparks giving barely usable results.

B. OPERATION OF VACUUM SPECTROGRAPH

Vacuum system operation is described in Appendix B. Alignment of the optical system with the central core of the plasma column was possible through trial and error exposures. A small degree of anastigmatism allowed centering of the spectral lines. The vacuum coupling of the spectrograph to the plasma system was modified to allow coupling at each of the five ports along the plasma column. Exposures were made for varying background pressures as set by varying the gas supply pressure. Exposure times ranged from thirty seconds at Port #1 (nearest the cathode) to ten minutes at Port #5 (next to the floating anode), for comparable results. Modification of the plasma vacuum system restricted the location of the spectrograph to Port #3, the plasma midpoint. At this port studies were made of the nitrogen plasma at magnetic field strengths from 2400 to 6000 gauss with the mirror magnet set to 1000 amps (5600 gauss) or turned off. Visible intensities increased at lower magnetic field strengths with the mirror magnet on, as expected.

C. SPECTRAL ANALYSIS

Calibration of the nitrogen spectrum was accomplished by comparison with previously identified helium spectra taken on the P-4 device and on the NPGS reflex arc. A sufficient number of lines was identified to allow fitting of the remaining comparator-determined positions to a

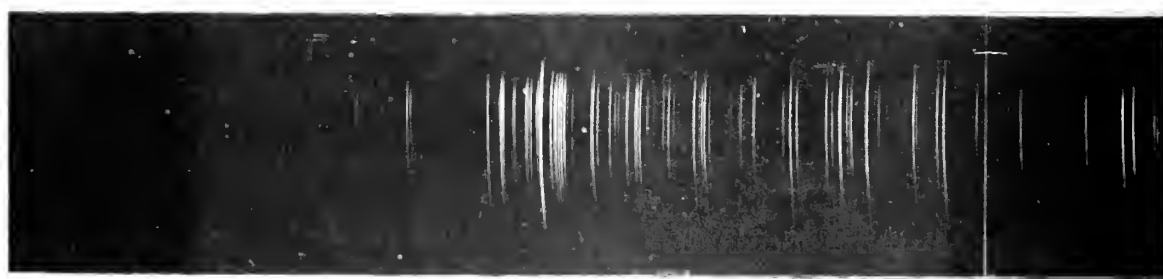
six degree polynomial. The nitrogen-helium spectrum is shown in Fig. 12 with complete identifications presented in Appendix C. Cross reference to this spectrum allowed identification of the nitrogen spectrum shown in Fig. 13 with identifications in Appendix D. For information only, argon spectra are shown in Fig. 14 from the previous and present gratings. Some improvement in sensitivity with the new grating is noted although relative exposure data are not available.

Density information was obtained by scanning the film with a Leeds and Northrup recording microphotometer using a Speedomax recorder. The density data were utilized in calculating electron temperatures by converting the data to intensities with an equation given by Harrison, Lord, and Loofbourov [15],

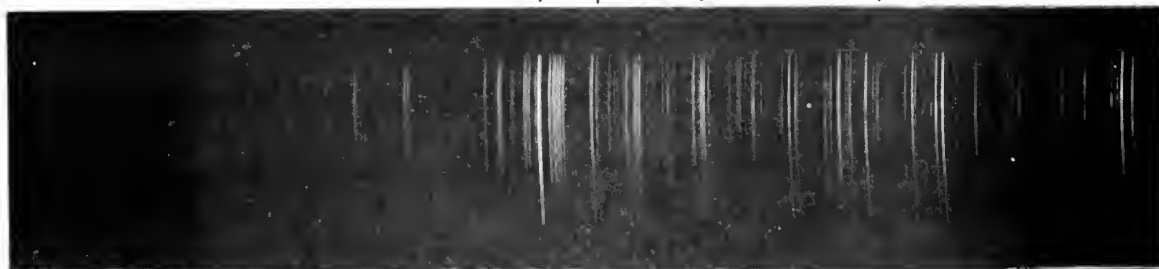
$$I_2 = I_0 \text{ antilog}_{10} [(D_2 - D_0)/\gamma]$$

where γ is the contrast of the photographic emulsion measured by the tangent of the density versus log intensity curve (commonly called the "H & D" curve). For the conditions under which the Kodak SWR film was used, gamma is estimated to be 1.6 for monochromatic exposure at 758 Å [16]. This estimate is based on the Kodak published density-log intensity curve, not on any published SWR gamma tabulations.

Background studies of nitrogen in preparation for the spectral survey included drawing of Grotrian diagrams for NI, NII, NIII, and NIV. The source for atomic energy levels was principally C. E. Moore [17]. Transition data were obtained from Moore [18], Kelly [19], Wiese, Smith, and Glennon [12] with supplementary references mentioned by these sources checked. Emphasis was given to vacuum ultraviolet transitions although prominent visible transitions between many of the lower lying levels are included. The diagrams are presented in Appendix 1.



Grating ↑ Uncoated ↑
 508 Ar III ↓
 475 Ar VII ↓ 573 Ar II ↓ 671 Ar II ↑ 690 Ar III ↓ 801 Ar IV ↑



Platinum Coated



↑ Uncoated ↑
 2 475 Ar VII ↓ 1215 He II ↓



Coated

FIG. 14

ARGON SPECTRA

D. PLASMA SYSTEM OPERATION

A number of problems remain unresolved with respect to operation of the plasma system. Lifetime of the hollow cathode has not improved with modification of the cathode assembly. Average lifetime of five cathodes used since completion of the new assembly was 8.03 hours as compared with an average lifetime in the old system of 10.0 hours. Failure of the cathode with one exception has occurred approximately 1.5 cm from the tip, suggesting reflected bombardment of the outside of the cathode or magnetic focusing at this point. Evaluation of the cathode life with anode magnet off operation is not complete. The first cathode used in this manner lasted for 20.37 hours, and appeared to be in excellent condition at 14.00 hours with a very slight ablative necking down over the first 1.5 cm of the cathode. It is expected that operation in this mode will substantially improve the cathode lifetimes. Reasons for using the anode-off operation are discussed in the following paragraph.

Although nitrogen plasma instability problems were not apparent in the new vacuum system, the entire plasma column was very diffuse with diametric extent of 8 cm. It was discovered by the author that operation of the system with the anode magnets off increased the stability of the plasma, narrowed the beam diameter to 1 cm, and greatly increased visible intensities. Alignment of the anode magnets on the plasma system longitudinal axis and magnetic field direction were checked and found to be in order. A possible explanation of this phenomenon may be a mirroring effect which results in major plasma confinement between the cathode and the fixed anode. Additionally, improper focusing of ions at the cathode would have a disruptive effect

on the entire beam. Background pressures measured with an ionization gauge above Port #3 indicate an increase of neutral pressure from 3.8×10^{-5} mm Hg to 1.2×10^{-4} when the anode magnet is energized.

E. THETA-PINCH SHOCK WAVE STUDY

Operation of the theta-pinch shock perturbation experiment installed on the plasma system was first achieved on 6 May 1969. The pulse was triggered initially with the plasma chamber at atmospheric pressure. Visual observations were made with the plasma arc not in operation at pressures from 100 microns to 0.5 microns. Observation of the plasma column with the shock pulse in operation is presently being conducted. Diagnostics used to date with both plasma system and shock perturbation in operation include; 1) visual observation of the plasma column for large scale intensity variation, 2) scanning of spectral lines with photomultiplier tubes at the exit slit of a dual beam monochromator, 3) oscilloscope investigations with photomultiplier tubes at the plasma system and isolated by use of light pipe, 4) Langmuir probe analysis, 5) comparison spectra produced by the vacuum ultraviolet survey spectrograph. Results are reported in the next section.

IV. OBSERVATIONS AND RESULTS

A. NITROGEN PLASMA SPECTRUM

Identifications of 735 lines were made from the nitrogen-helium spectrum and are reported in Appendix C. Of these the more intense nitrogen lines arise from NIII, with NII secondary in numbers and intensities of lines. No attempt has been made to correct the intensities for spectral sensitivity variation of the film or spectrograph. It is noted that there is a general diminishing of the number and intensity of spectral lines below 400 \AA and above 1600 \AA . Resonance lines of NV, 1238.821 and 1242.804 , appear on the nitrogen-helium spectrum, but not on the nitrogen spectrum. This result most likely arises from an energy transfer from helium ions and electrons in the helium plasma to nitrogen contaminants. In the nitrogen plasma this energy might be self-absorbed by the lower lying species NII and NIII, or dissipated in collisional recombination. Of nitrogen's seven ionization states, NI, NII, NIII, NIV, and NV are believed to have been observed. Impurities included carbon, oxygen, argon, and possibly helium and silicon.

B. RELATIVE LINE INTENSITIES

In an effort to establish a radiation model for the plasma, both the Local Thermal Equilibrium model and the Corona model were linearly combined. With temperature inputs from 4.0 eV to 8.0 eV , markedly different intensities were calculated for LTE versus Corona models. Results for a group of 21 lines in the range 529.4 \AA to 672.0 \AA are shown in the table on the following page. The intensities show slight sensitivity to variation in model and pronounced sensitivity to changes

RELATIVE LINE INTENSITY RADIATION MODEL MIX RESULTS

WAVELENGTH	LTE	INTENSITIES FROM MODEL MIX				CORCNA
		80%LTE	60%LTE	40%LTE	20%LTE	
671.800E-10	45.263	55.059	64.854	74.650	84.446	94.242
671.600E-10	33.785	41.074	48.362	55.651	62.940	70.229
671.959E-10	56.208	68.334	80.460	92.587	104.713	116.840
671.400E-10	44.943	54.630	64.335	74.032	83.728	93.424
671.400E-10	166.863	202.750	238.636	274.522	310.408	346.295
671.000E-10	55.529	67.472	79.414	91.357	103.299	115.241
747.000E-10	233.859	283.837	333.816	383.794	433.773	483.752
533.600E-10	264.322	237.949	211.576	185.204	158.831	132.458
533.500E-10	117.333	106.077	94.320	82.563	70.806	59.049
533.800E-10	88.718	79.619	70.795	61.970	53.146	44.321
533.600E-10	491.371	79.866	71.014	62.162	53.311	44.459
533.700E-10	121.428	442.281	393.190	344.100	295.010	245.919
582.200E-10	136.942	109.376	97.324	85.271	73.219	61.167
529.900E-10	110.553	33.176	29.409	25.643	21.877	18.110
529.500E-10	21.790	99.281	88.010	76.739	65.468	54.197
529.700E-10	36.360	19.565	17.341	15.117	12.893	10.668
529.400E-10	28.950	32.937	28.937	25.225	21.514	17.802
529.300E-10	29.052	25.994	23.039	20.084	17.129	14.174
574.700E-10	477.549	26.086	23.120	20.155	17.189	14.224
635.200E-10	100.000	428.861	379.773	330.685	281.598	232.510
		89.606	79.211	68.817	58.423	48.028

Electron Temperature = 4.0 eV

INTENSITIES FROM MODEL MIX

WAVELENGTH	LTE	80%LTE	60%LTE	40%LTE	20%LTE	CORCNA
671.800E-10	23.9047	29.141	34.326	39.510	44.695	49.880
671.600E-10	127.9047	221.766	25.629	29.492	33.354	37.918
671.400E-10	238.8177	36.213	42.639	49.065	55.491	61.509
671.400E-10	89.5374	28.555	34.094	39.232	44.370	49.747
671.000E-10	124.3496	107.579	126.620	145.661	164.702	183.747
671.000E-10	253.3411	135.880	177.566	204.474	230.810	257.147
533.600E-10	1253.0720	150.334	203.027	277.151	330.413	391.106
533.500E-10	1134.0703	101.402	90.508	179.227	227.945	277.630
533.300E-10	872.1334	76.633	67.173	59.466	50.998	42.567
533.300E-10	472.1040	424.438	377.927	330.608	283.910	236.277
529.200E-10	1136.2111	104.516	92.827	81.417	69.442	58.403
529.600E-10	108.3365	97.316	86.268	75.135	64.442	53.752
529.500E-10	21.3385	19.202	17.019	14.836	12.653	10.470
529.700E-10	328.6412	32.042	28.399	24.757	21.172	17.472
529.400E-10	28.5122	25.510	22.691	19.711	16.811	13.911
529.300E-10	472.5012	25.534	22.691	19.711	16.811	13.911
574.700E-10	100.000	489.606	375.056	326.578	278.100	228.522
635.200E-10			79.211	68.817	58.423	48.028

Electron Temperature = 8.0 eV

in electron temperature. As the model approached 100% Corona, relative intensities doubled in most cases. With increasing electron temperature, the relative intensities decreased but not as sharply as with model variation.

The most obvious use of the calculations or similar ones in the visible spectrum is to determine which radiation model is more appropriate for any given ion species. To accomplish this an accurate independent measurement of electron temperature must be made. Intensities from the model mix calculations should then pinpoint the correct model, or show that a certain linear combination gives satisfactory results. A further result would of course be more accurate determination of absorption oscillator strengths.

Another possible use of the model mix is for intensity predictions over a wide wavelength range. The drawback to accurate intensity predictions at the present time is again lack of precise values for the absorption oscillator strength.

C. ELECTRON TEMPERATURE EVALUATION

Initial results from density information in the vacuum ultraviolet produce wide variation in electron temperature. Values were uniformly spread over a range of 1.0 eV to 12.0 eV. Work is continuing in this area, although oscillator strengths in the vacuum ultraviolet region may vary as much as 40-50% even within the same multiplet.

The preliminary VUV density results prompted further investigation in the visible region. Using the unpublished intensity measurements made by Major J. Cote using a dual beam spectrophotometer, electron temperatures were calculated using the Corona model. The results for various magnetic field strengths are presented below.

<u>Magnetic Field</u>	<u>LTE</u>	<u>CORONA</u>
2400 gauss	3.8473 eV	7.3384 eV
3000	3.8650	7.3725
3600	5.5496	19.663
4200	measurements	inconsistent
4800	4.4115	9.7736

It is believed that the Corona values are more nearly correct in view of the large violation of the LTE validity criterion. The value for 3600 gauss is questionable in view of the tendency of the electron temperature equation to become indeterminate for very small values of the logarithmic term in the denominator.

D. THETA-PINCH PERTURBATION

No visible effects have been noted on the plasma column due to the theta-pinch discharge. Ionization of both argon and nitrogen has been achieved with the chamber pressure between 100 microns and 4.8×10^{-4} mm Hg. Below this pressure, effects of the shock pulse were not seen with the reflex arc off.

Attempts to observe the shock with the spectrophotometer were equally unrewarding. Minor oscillations were determined to be extraneous pickup of the trigger signal in the pressurized spark gap switch. RF discharge has been noted at all locations in the plasma laboratory including sparking between wires of a diagnostic coil placed near the single coil theta-pinch device. Attempts to filter the RF signal are in progress. Probe signals showed pickup of the trigger signal but no useful information on perturbations within the plasma column.

The first possible indication of variation of the plasma column was picked up on 19 May 1969, by a remote photomultiplier connected to the plasma tube by a light pipe. The signal to the oscilloscope was

directly related to the spark of the trigger gap although the signal was not noted every time the spark trigger indicated discharge through the theta-pinch coil. The signal showed a rise time of slightly less than 1 microsecond and an amplitude approximately 2.5 times the noise amplitude. Confirmation that the signal was indeed from the plasma was based on complete shielding of the light flash from the trigger spark (signal still received) and closing of the photomultiplier shutter (signal off). The rise time corresponds to design predictions of a one megacycle frequency for the discharge. That the shock front cannot be seen visibly in spite of the size of the signal may be attributed to the speed of the shock front estimated at 10^7 cm/sec.

On verification that a perturbation existed within the plasma column, an attempt was made to observe the effect in the vacuum ultraviolet spectrum. Subsequent exposures under identical conditions of plasma operation showed no difference in the spectrum exposed during theta-pinch perturbation.

V. CONCLUSIONS AND RECOMMENDATIONS

A. SPECTROGRAPHIC ANALYSIS

Spectral survey of the nitrogen plasma in the vacuum ultraviolet was valuable because it was a previously uninvestigated area of the NPGS reflex arc spectral characteristics. Considerable information on the steady state plasma system must be available prior to attempting meaningful diagnostics on a shock-disturbed plasma.

Lack of concise electron temperature information from photographic intensities was partly expected. The large variation in the spectral response of SWR film, unknown wavelength-dependent response of the spectrograph, and lack of temperature control processing make quantitative spectral analysis difficult in this region. Values of absorption oscillator strength for transitions in the ultraviolet are known only within 40% at best. Expected electron temperatures are in the same range as the excitation potential difference, so any change of this magnitude in the logarithmic term would greatly alter the calculated electron temperatures. Some overlapping of spectral lines prevented utilization of certain wavelengths with recent oscillator strength values. From computer analysis it was determined that electron temperatures (or intensities for the inverse equation) are very sensitive to values of absorption oscillator strength and statistical weight.

Close agreement of photometric data with probe measured values appears reliable, although use should be made of the corona radiation model.

B. TIME RESOLVED PHOTOMETRY

There is a definite need for time resolved photometric observation of the plasma. This may be accomplished most easily by oscilloscope/spectrophotometer observation in the visible region. If observations establish that response is inadequate in this region, then consideration should be given to developing time resolution capability in the vacuum ultraviolet. Since the most intense lines occur in this region, response to perturbations should be larger. Experimental difficulties of work in the vacuum ultraviolet make complete quantitative spectral analysis in the visible spectral regions a first priority. Further investigations in the vacuum ultraviolet should be conducted only when it appears that spectral line intensities in the visible region are not sufficiently sensitive perturbation indicators.

C. VUV SCANNING MONOCHROMATOR

Difficulties in preventing contamination of bare photomultiplier tubes, and in scanning over the desired wavelength range make construction of a vacuum ultraviolet monochromator extremely difficult. Desire to maintain capabilities in the extreme vacuum ultraviolet requires grazing incidence. Any deviation of components of a grazing incidence spectrograph results in large scale defocusing. The most practical, although initially more expensive, solution is purchase of a commercially produced grazing incidence scanning monochromator. The returns from such an instrument would justify the expenditure. Of those instruments and designs investigated the McPherson 2 meter grazing incidence monochromator [19] appears to be the best design.

D. MAGNETIC FIELD SURVEY

It is imperative that a complete survey of the magnetic field of the plasma system be undertaken as soon as possible. Existing Hall probe measurements are inadequate and rather limited as to range of mirror, main, anode, and cathode field variation. Particular attention in the vicinity of the anode-cathode section would go far toward solving the anode magnet instability problem.

E. SPARK GAP SPECTRAL STUDIES

The remarkable improvement in the efficiency of the spark gap calibration source suggests its use for further spectral studies of the higher ionization states of all electrode materials. The simplicity of the design requiring only glass tubing and heavy gauge wire permits convenient phasing from one spectrum to another or operation with test electrode and calibration electrodes together.

APPENDIX A

PLASMA OPERATING INSTRUCTIONS

I. Evacuate Chamber

A. Evacuate Foreline:

1. Preliminary checklist:

- a. Control power Ckt 25 ON
Air interlock switch ON
Water interlock sw ON
Mode switch START FOREPUMP
Foreline relay meter - Set at 30 u
- b. Check compressor air pressure at approx. 70 psi (CAGE).
- c. Check following valves CLOSED:

V2 through V6 (Gate valves)
Foreline vent valve
Booster manifold vent valve
Foreline gate valve to 10" DP
- d. Check the following valve OPEN: V7 (Booster gate valve).
- e. Check system water valve OPEN: Pressure approx. 40 psi.
- f. Check forepump water valve OPEN at forepump (identified by wire looped through handle). Adjust for slow steady stream of water.

2. Press Forepump START button at the control wall. Foreline and Booster manifold pressures should drop to 20 u in approx. two (2) minutes.

3. Set booster relay meter at 500 u.

4. When forepump relay meter has locked, press forepressure interlock button. The interlock light should glow.

5. Turn Mode switch to RUN FOREPUMP position.

B. Pump Out Chamber (Rough Pumping/High Vac)

1. Check boiler cooling water to 10" DP OFF.

2. Turn ON Ion Gauge Controller Power & Stand-by Control Power.

I. Evacuate Chamber (continued)

3. Open manual throttle valve at machine.
- 4A. If chamber is at atmospheric, with DP's OFF:
 - a. CLOSE V7 & V6.
 - b. Close manual throttle valve.
 - c. Open V6.
 - d. Gradually open manual throttle and observe forepump exhaust for normal levels of water vapor.
 - e. Pump down to 80 u.GO TO STEP 5 IMMEDIATELY!
- 4B. If chamber is at atmospheric, with DP's ON:
 - a. Complete steps in 4A, but leave mode selector switch on START DP's & REFRIG.
 - b. GO TO STEP 5 IMMEDIATELY, BUT OMIT STEPS 9, 11.
- 4C. If chamber is at 500 u, with DP's OFF:
 - a. Close V7, Open V6, Pump down to 80 u, (indicated on TC2).
 - b. GO IMMEDIATELY TO STEP 5.
5. OPEN V7.
6. START Argon purge at cathode to maintain 80 u (TC2) -
Note: usually wide open on the argon needle valve.
7. OPEN foreline 10" DP Gate Valve, CLOSE V6.
8. Check water flow to 10" DP: Boiler cooling OFF; DP Inlet, DP Outlet, Baffle Cooling ON.
9. Procedure for starting diffusion pumps (DP's) and refrigeration:
 - a. Check Refrigeration Toggle switch OFF.
 - b. DP Toggle switches may be left ON.
 - c. Turn Mode Selector switch to START DP's & REFRIG.
10. Turn 10" DP Heater ON.

I. Evacuate Chamber (continued)

11. Individual DP Heater switches may now be turned ON (if not already ON).
12. Record starting time in Vacuum Log.
13. Turn Refrigeration Toggle switch ON. Allow approximately ten (10) minutes for cooling.
14. Allow twenty (20) minutes for warm-up.
15. When chamber pressure begins to drop (indicating DP's pumping), secure the Argon purge and note the time. Pressure should drop to less than 1 u.
16. Set Booster Relay to 100 u. Press baffle interlock button.
17. High vacuum procedures may be commenced when the 10" DP has started pumping. Check that the following conditions exist prior to high vacuum pumpdown:
 - a. Ion gauge controller power ON, pressure multiplier at 10^{-4} .
 - b. Chamber pressure should be below 1 u.
 - c. Ion gauge standby control power ON, filament toggle switches in ON positions (as needed), Outgas switches OFF.
 - d. Start ion gauge by simultaneously pressing:
 1. Filament ON (Ion gauge controller)
 2. Reset (Ion gauge standby controller)
 - e. The diffusion pumps (DP's) should have heated at least twenty minutes. Check cooling water temperatures.
 - f. Baffle signal light (interlock) should be ON.
 - g. Check V6 CLOSED, V7 OPEN.
18. If these conditions exist, OPEN valves V2 through V5, and note time in the Vacuum Log. If the opening of any valve causes a pressure rise allow more warm-up time for that diffusion pump with the valve closed.
19. Record pressures/time at 1 min, 2 min, 4 min, etc., and plot on log-log coordinates in order to judge the condition of the pumpdown and freedom from leaks. The zero (starting) time will be taken as the time when the argon purge is secured.

20. Turn Mode Selector switch to RUN DP's & REFRIG for operation protected from pressure rise. A pressure exceeding $1.5 \times$ the full scale ion gauge reading will cut OFF the ion gauge, ion gauge standby control, close valves V2 through V5, and cut OFF the DP's.

II. Magnet and Arc Operating Procedures

A. Preliminary

1. Set Booster Relay to 500 u.
2. Start Argon gas flow to the cathode, set initially at 3×10^{-4} .
3. Fill pure water:
 - a. Close de-ion loop valve.
 - b. Open main water valve $3/4$ to 1 turn and fill until overflow observed.
 - c. Secure main water valve.
 - d. Reopen de-ion loop valve.
4. Turn OFF Ion Gauge #4 (Reflex Anode)
5. Remove watches, warn personnel, inspect for tools lying around machine.

B. Energize magnets:

1. Connect blower at reflex anode.
2. Start Pure Water followed by Raw Water. Allow two minutes for stabilization of pressures.
3. START cooling tower. Check to ensure its operation.
4. Observe water flow in all flow meters and check hoses for flow and leaks.
5. Turn ON Control Power CKT 21, Push 3 interlock buttons.
6. START Control Power CKT 19 (if it kicks out, reset circuit breaker, then restart).
7. START Control Power CKT 23. (Both CKT's 19, 23 usually left ON).
8. Turn Mirror Magnet Rectifier Power switch ON (located in shed nearest the door).

II. Magnet and Arc Operating Procedures (continued)

9. START other rectifiers by turning ON Standby switch at console. The operation of the rectifiers is verified by the roar of the rectifier fans.
10. Consult magnet chart for operating conditions to give desired field, switch ON appropriate number of units at the console. Have been starting with #3 ON, rheostat at 65% to give 400 amps in the main magnets.
11. Press START buttons to start magnet current (separate buttons for mirror, main, anode, and cathode magnets).
12. Record time of start in Magnet Log Book.

C. Energize Arc

1. Start R-F. If not observed increase pressure until it is observed.
2. Press both Arc - ON buttons simultaneously.
3. On start, immediately reduce #2 Anode Voltage Control rheostat to obtain an arc current of 60 amps.
4. Remove R-F.
5. Adjust magnet fields, supply flow, as needed - reset anode voltage control for arc current 60 amps.
6. To switch to another gas, OPEN other needle valve until flow observed on the ion gauge, then continue opening while securing the Argon needle valve.

III. Shutdown Procedures

A. Arc and Magnets:

1. Arc OFF.
2. Main, mirror, anode, cathode magnets OFF.
3. Secure gas flow.
4. Control Power CKT 21 OFF.
5. When all water cooling return lines are cool (check anode magnets in particular); a) Secure cooling tower, b) Raw Water OFF, c) Pure Water OFF.
6. Standby Switch OFF (Secures rectifier fans).

III. Shutdown Procedures (continued)

7. Turn Mirror Magnet Rectifier Power switch OFF (located in shed, nearest door).
 8. Reflex anode blower OFF.
 9. Lock cooling tower cage.
- B. Chamber - Secure to 500 u with overnight defrost. If desirable to bring chamber to air, see Section III C.
1. Set Mode Selector Switch to START DP's & REFRIG.
 2. Close gate valves V2 through V5.
 3. START Argon flow - open to 80 u as indicated to the Booster Relay TC (usually wide open).
 4. 10" DP Heater OFF.
 5. Open Booster Cooling Water valve - Note time.
 6. Refrigeration switch OFF.
 7. DP Heaters OFF.
 8. Mode selector switch to RUN FOREPUMP.
 9. Wait 10 minutes after TC2 indicates pumping action stopped.
 10. CLOSE 10" DP Gate Valve.
 11. Secure Argon flow at 500 u.
 12. System is now shutdown for overnight with defrost. To pump down from this condition, start at I-B-1 using part I-B-4C.
- C. Chamber - Secure chamber to atmospheric with vacuum maintained on booster manifold.
1. Set Mode Selector switch to START DP's & REFRIG.
 2. CLOSE gate valves V2 through V5.
 3. Start Argon purging flow - open to 80 u on Booster Relay TC (Argon needle valve usually wide open).
 4. Turn 10" DP Heater OFF.
 5. OPEN Boiler Cooling Water valve - Note Time.

III. Shutdown Procedures (continued)

6. Wait for 10 minutes after TC2 indicates pumping action stopped.
7. CLOSE Foreline Gate Valve to 10" DP.
8. Start main nitrogen purging through system vent valve.
9. Secure Argon purge through cathode.
10. Secure vent valve when manometer indicates atmospheric.
11. Secure nitrogen vent supply.
12. System is now in condition of temporary secure. Work on chamber and related components now possible. To pump down from this condition, start at I-B-1, using part I-B-4B. If it is desired to go ahead and secure the DP's proceed to the next step.
13. Turn OFF Refrigeration toggle switch.
14. Turn OFF DP Heaters.
15. Move Mode Selector switch to RUN FOREPUMP.
16. Set Booster Relay meter to 100 u.
17. Chamber is now in condition of temporary secure with DP's and Refrigeration OFF. To pump down from this condition start at I-B-1, using part I-B-4A. If complete shutdown is desired proceed to the next step.
18. Turn OFF Forepump. System is self venting. If immediate venting desired, OPEN Foreline Vent valve.

APPENDIX B

VUV SPECTROGRAPH OPERATION

A. Vacuum Procedures.

1. Operation with roughing pump only:
 - a. Check all valves closed; pressures equalized.
 - b. Power to all circuits.
 - c. Thermocouple ON.
 - d. If operating with spark gap, open shutter valve 1/2 open.
If operating with plasma, leave valve closed. Insert film and secure back plate.
 - e. Start forepump.
 - f. Open red handle throttle valve.
 - g. Pump down to approximately 50 microns (about 5 min.)
 - h. UV Spectrograph vacuum system is now ready for spark gap operation.
2. Operation with roughing and diffusion pumps.
 - a. Complete steps as listed above.
 - b. Connect water inlet and drain.
 - c. Connect ion gauge - commence warm-up.
 - d. At approximately 50 microns:
 - (1) Close roughing valve.
 - (2) Open foreline valve.
 - e. Turn ON diffusion pump.
 - f. Warm-up 20 minutes.
 - g. Fill IN Trap 2/3 full (about 3 liters).
 - h. Turn ion gauge ON.
 - (1) Set pressure range selector to 10^{-4} .
 - (2) Adjust zero.

VUV SPECTROGRAPH OPERATION (continued)

- (3) Gauge filament ON.
- (4) Meter selector to I_g - adjust I_g to 1 ma.
- i. Close foreline valve.
- j. Open roughing valve. Pump down to 10 microns.
- k. Close roughing valve.
- l. Open foreline valve.
- m. Open DP Gate valve.
- n. System is now ready for full vacuum operations.
If the plasma system is under comparable vacuum, the shutter gate valve may be opened as desired for exposures.
- o. To recycle films with plasma and VUV systems in operation:
 - (1) Close shutter valve.
 - (2) Close DP gate valve.
 - (3) Vent chamber of VUV Spectrograph to atmosphere.
 - (4) Change films.
 - (5) Secure vent, close foreline valve.
 - (6) Open roughing valve to rough down chamber to 100 microns.
 - (7) Close roughing valve.
 - (8) Open foreline valve. Check that foreline is at 10 microns or less.
 - (9) Open DP gate valve.
 - (10) System is now ready for further exposures.

APPENDIX C

NITROGEN - HELIUM SPECTRUM

Wavelength (Å)	Identification	Wavelength (Å)	Identification
197.230	N IV	282.213	N III
205.960	N IV	283.579	N IV
225.136	N IV	284.346	N III
225.205	N IV	289.230	C IV
230.139	H• II	291.054	O IV
230.686	H• II	291.263	O IV
231.454	H• II	291.326	C III
232.584	H• II	292.447	N III
234.347	H• II	292.595	N III
237.331	H• II	294.650	O IV
238.361	O IV	295.657	O III
238.573	O IV	296.012	O III
239.618	N IV	296.951	C IV
240.979	O III	297.815	N IV
241.037	O III	299.820	N III
243.027	H• II	303.783	H• II
244.049	O III	303.891	N III
244.907	C IV	303.981	N III
247.205	N IV	304.032	N III
248.538	O III	304.818	N III
248.574	O III	304.874	N III
248.618	O III	304.912	N III
256.317	H• II	305.596	O III
256.425	O III	305.656	O III
256.460	O III	305.703	O III
256.506	O III	305.769	O III
259.542	C IV	305.836	O III
260.455	N IV	305.879	O III
261.027	O III	305.918	N III
263.818	O III	310.1697	C III
264.480	O III	311.628	N III
264.837	N III	312.422	C IV
266.985	O III	312.453	C IV
267.030	O III	314.715	N III
268.451	O III	314.850	N III
270.583	C III	314.877	N III
272.125	O IV	315.053	N IV
272.311	O IV	319.266	C III
274.051	C III	320.392	H• I
275.513	O III	320.979	O III
277.385	O III	321.161	N III
280.043	C III	322.503	N IV

Wavelength (Å)	Identification	Wavelength (Å)	Identification
322.570	N IV	374.165	O III
322.5741	C III	374.204	N III
322.724	N IV	374.331	O III
323.431	N III	374.436	O III
323.488	N III	374.441	N III
323.615	N III	377.045	O III
323.671	N III	379.574	O III
327.112	C III	384.178	C IV
327.176	C III	384.032	C IV
328.448	O III	387.353	N IV
328.742	O III	388.9687	C III
332.133	N III	389.0045	C III
332.327	N III	389.0898	C III
335.050	N IV	391.943	O II
341.143	C III	392.002	O II
341.179	C III	392.322	O II
341.242	C III	395.558	O III
345.063	N IV	397.120	O III
345.309	O III	398.885	N III
347.777	C III	399.045	N III
347.854	C III	399.084	N III
351.979	N III	399.637	C III
358.327	N III	399.688	C III
358.578	N III	403.273 ?	O II ?
358.740	C III	409.325	C III
359.016	O III	411.9577	C III
359.223	O III	418.705	N III
359.384	O III	418.910	N III
360.557	C III	419.525	C IV
360.623	C III	419.714	C IV
360.675	C III	425.273	O II
362.833	N III	426.526	O II
362.881	N III	428.180	N III
362.946	N III	428.244	N III
362.985	N III	429.557	O II
363.7538	C III	429.647	O II
363.7852	C III	429.716	O II
363.8598	C III	430.041	O II
364.739	O III	430.177	O II
366.169	C III	433.3391	C III
369.415	C III	433.911	N III
371.694	C III	434.014	N III
371.747	C III	434.066	N III
371.784	C III	434.129	N III
373.805	O III	434.256	O III
374.005	O III	434.246	N III
374.075	O III	434.280	N III

Wavelength (Å)	Identification	Wavelength (Å)	Identification
434.646	O III	475.884	N II
434.840	O III	476.43	Ar III
434.975	O III	477.6246	C III
436.510	O II	480.955	O III
436.649	O II	481.354	O III
437.332	O II	481.381	O III
437.683	O II	482.548	Ar III
440.552	O II	483.567	C III
440.598	O II	483.618	C III
442.001	O II	483.733	C III
442.048	O II	483.976	O II
443.42	Ar ?	484.025	O II
445.601	O II	484.116	Ar III
445.638	C II	484.445	Ar III
446.949	Ar V ?	485.086	O II
447.527	Ar V ?	485.465	O II
449.065	Ar V ?	485.515	O II
449.493	Ar V ?	485.572	O II
450.079	Ar V ?	485.631	O II
450.44	Ar ?	487.025	Ar III
450.7338	C III	487.988	Ar III
451.20	Ar IV?	488.452	Ar III
451.869	N III	489.195	Ar II
452.226	N III	492.6500	C III
452.91	Ar IV ?	493.341-.587	C III
452.92	Ar ?	495.55	Ar
453.340	N II	406.91	Ar
456.078	N III	499.425	C III
456.997	O II	499.583	C III
459.462	C III	499.871	O II
459.521	C III	500.343	O II
459.633	C III	501.01	Ar
460.0487	C III	505.986	N II
462.415	Ar V ?	506.153	N II
463.737	N IV	506.054	N II
464.785	O II	507.391	O III
466.491	C II	507.683	O III
466.9	Ar ?	508.182	O III
468.766	O II?	508.6341	H● I
470.408	O II	508.697	N II
472.232	N III	509.586	N III
472.392	N III	509.897	N III
473.025	Ar III	510.758	N II
473.918	Ar III	511.523	C III
474.891	N II	512.0982	H● I
475.647	N II	2 x 256.317	H● I
475.698	N II	514.3097	Ar II
475.803	N II	515.498	O II

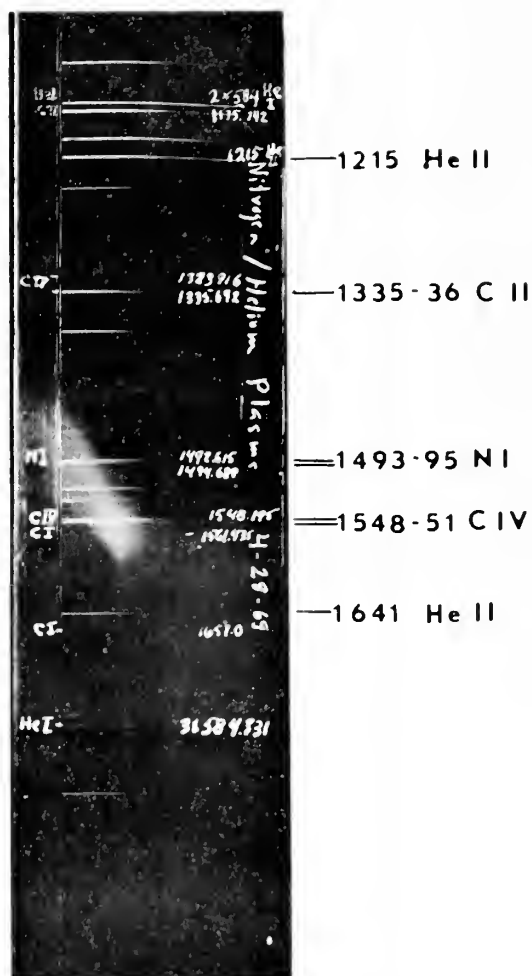
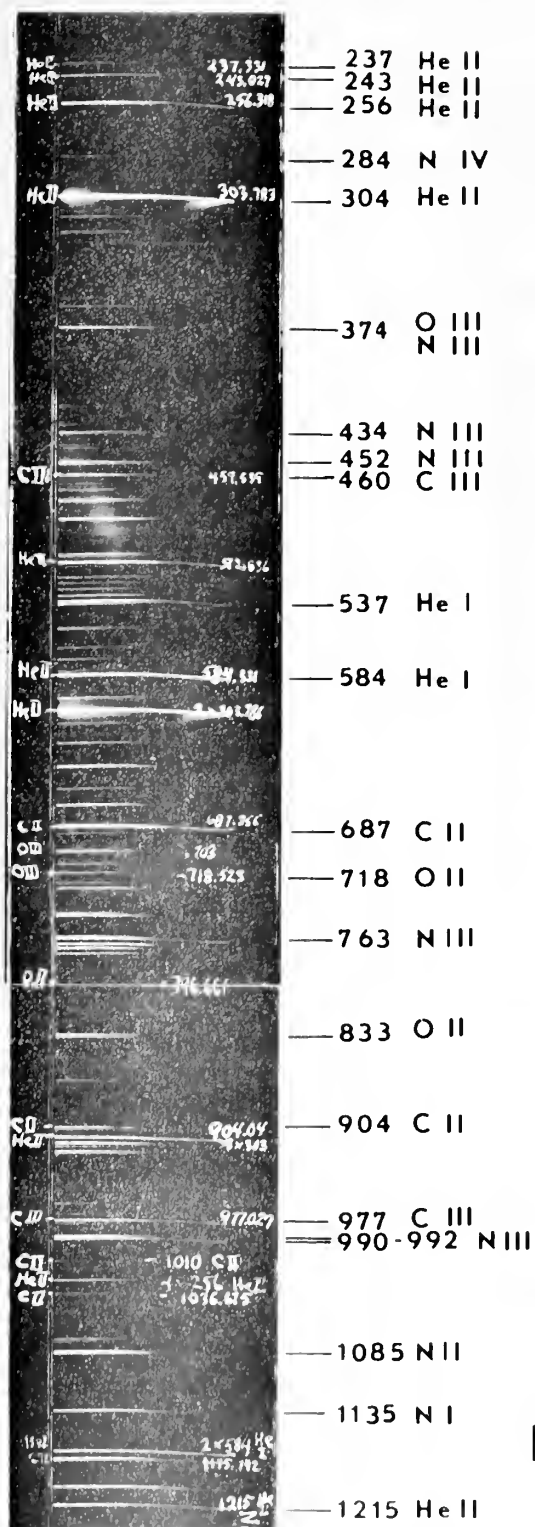
Wavelength (Å)	Identification	Wavelength (Å)	Identification
515.6165	H α I	555.056	O II
515.640	O II	555.121	O II
517.937	O II	555.262	O IV
518.242	O II	556.8172	Ar II
522.2128	H α I	556.893	Ar III
524.189	Ar V	558.321	Ar III
525.795	O III	559.48	Ar
527.693	Ar V	559.762	N II
528.6508	Ar II	560.2394	C II
529.355	N II	560.4367	C II
529.413	N II	564.608	C II
529.491	N II	564.663	C II
529.637	N II	565.5280	C III
529.722	N II	2 x 283.420	N IV
529.867	N II	2 x 283.470	N IV
530.037	N III	2 x 283.579	N IV
530.268	N III	572.069	N II
532.659	C II	573.3622	Ar II
532.705	C II	573.468	Ar III
533.511	N II	574.2809	C III
533.581	N II	574.650	N II
533.650	N II	574.799	Si III ??
533.729	N II	578.1068	Ar II
533.815	N II	578.386	Ar III
535.0713	Ar II	579.212	Ar III
535.2885	C III	580.2634	Ar II
535.580	Ar III	580.400	O II
536.745	Ar III	580.967	O II
537.0296	H α I	582.156	N II
537.830	O II	584.334	H α I
538.0801	C III	585.261	C III
538.1487	C III	585.417	C III
538.318	O II	585.496	C III
539.086	O II	585.608	C III
539.547	O II	585.666	C III
543.444	C II	591.4117	H α I
546.1770	Ar II	594.8000	C II
547.4602	Ar II	595.0219	C II
548.7810	Ar II	595.0245	C II
549.3195	C II	597.818	O III
549.3785	C II	599.598	O III
549.5110	C II	600.251	C II
549.5700	C II	600.337	C II
551.874	C II	600.353	C II
553.328	O IV	600.503	C II
554.074	O IV	600.518	C II
554.514	O IV	600.585	O II
554.655	C III	601.468	N III

Wavelength (Å)	Identification	Wavelength (Å)	Identification
601.878	N III	673.768	O II
602.8581	Ar II	679.4001	Ar II
604.152	Ar II	683.278	Ar IV
2 x 303.783	H β II	684.996	N III
608.395	O IV	685.513	N III
609.275	C III	685.816	N III
609.705	O III	686.416	C II
610.043	O III	686.488	C II
610.746	O III	687.0526	C II
610.850	O III	687.345	C II
616.291/616.363	O II ?	687.352	C II
617.051	O II	689.007	Ar IV
622.144	C III	690.170	Ar III
624.617	O IV	690.526	C III
625.130	O IV	691.187	N III
625.852	O IV	691.388	N III
629.167	N II	695.537	Ar III
629.447	N II	697.4893	Ar II
629.732	O V	697.9414	Ar II
635.197	N II	700.277	Ar IV
635.9945	C II	702.332	O III
636.2511	C II	702.822	O III
637.282	Ar III	702.899	O III
641.888	C II	703.850	O III
644.148	O II	704.5233	Ar II
644.634	N II	709.195	Ar V
644.837	N II	713.518	N V
645.178	N II	713.860	N V
651.211	C II	716.55	O V
651.234	C II	718.0903	Ar II
651.269	C II	718.484	O II
651.304	C II	718.562	O II
651.345	C II	723.3611	Ar II
651.389	C II	725.5481	Ar II
657.327	N II	728.74	O V
658.578	O III	730.9293	Ar II
659.538	O II, N II	739.949	O II
660.286	N II	740.2695	Ar II
661.8692	Ar II	744.9252	Ar II
664.5626	Ar II	745.841	N II
666.0112	Ar II	746.984	N II
670.296	N II	748.291	N V ?
670.515	N II	748.4	O I
671.016	N II	749.3	O I
671.411	N II	752.762	O III
671.773	N II	756.7	O I
672.001	N II	759.440	O V
672.948	O II	760.445	O V

Wavelength (Å)	Identification	Wavelength (Å)	Identification
763.340	N III	836.279	N II
764.357	N III	836.289	N II
765.148	N IV	836.616	N II
769.152	Ar III	836.627	N II
769.355	O I	836.837	N II
769.411	O I	2 x 418.705	N III
770.264	O I	2 x 418.910	N III
770.350	O I	843.772	Ar IV
771.544	N III	850.602	Ar IV
771.901	N III	858.0918	C II
772.385	N III	858.5590	C II
772.891	N III	866.805	Ar I
772.975	N III	871.099	Ar III
774.522	O V	884.516	C III
775.965	N II	888.019	N I
2 x 389	C III ?	888.363	N I
778.172	N V	894.310	Ar I
783.14	Ar	898.957	O III
784.393	C III	901.168	Ar IV
787.710	O IV	901.804	Ar IV
790.103	O IV	903.6235	C II
790.203	O IV	903.9616	C II
791.974	O I	904.1416	C II
792.233	O I	904.4801	C II
792.507	O I	905.829	N I
795.134	C II	906.722	N I
796.661	O II	906.824	N I
799.660	C II	909.6976	N I ?
799.944	C II	910.2785	N I ?
802.198	O IV	910.6456	N I ?
802.250	O IV	915.612	N II
806.384	C II	915.962	N II
803.533	C II	916.012	N II
806.568	C II	916.020	N II
806.830	C II	916.701	N II
806.860	C II	916.710	N II
809.677	C II	919.7815	Ar II
811.052	O I	921.992	N IV ?
822.161	Ar V ?	922.519	N IV ?
827.052	Ar V ?	923.057	N IV ?
832.762	O II	923.220	N IV ?
832.927	O III	923.675	N IV ?
833.332	O II	924.283	N IV ?
833.742	O II	953.9698	N I
834.462	O II	954.1040	N I
835.096	O III	955.335	N IV
835.292	O III	958.670	H● II
836.187	N II	958.724	H● II

Wavelength (Å)	Identification	Wavelength (Å)	Identification
963.9904	N I	1097.245	N I
964.6258	N I	1098.264	N I
965.0415	N I	1100.3593	N I
971.7376	O I	1101.2910	N I
972.138	H ₂ II	1122.328	C I
973.2346	O I	1134.1651	N I
973.8857	O I	1134.4147	N I
976.4480	O I	1134.9801	N I
977.020	C III	1135.244	N IV
979.842	N III	1141.6246	C II
979.919	N III	1143.606	N I
989.790	N III	1143.6508	N I
991.514	N III	1149.603	O III
991.579	N III	1152.152	O I
992.334	H ₂ II	1156.028	C I
992.391	H ₂ II	1156.560	C I
999.493	O I	1163.8835	N I
1006.015	N III	1164.2064	N I
1008.875	N I	1164.3246	N I
1009.862	C II	1167.4484	N I
1010.092	C II	1168.3344	N I
1010.374	C II	1168.5358	N I
1025.241	H ₂ II	1169.6933	N I
1025.302	H ₂ II	1170.2766	N I
1025.7616	O I	1171.0834	N I
1027.4309	O I	1170.2766	N I
1028.1571	O I	1174.933	C III
1031.169	Si III ?	1175.711	C III
1032.958	N I	1176.370	C III
1033.453	N I	1176.5097	N I
1036.3367	C II	1177.6948	N I
1037.0182	C II	1183.030	N III
1044.094	N I	1184.544	N III
1044.724	N I	1188.006	N IV
1065.8913	C II	1193.240	C I
1065.9199	C II	1196.1	Si ?
1066.1332	O II	1199.5490	N I
1066.641	N I	1200.2238	N I
1067.399	N I	1200.7113	N I
1068.476	N I	1215.171	H ₂ II
1069.984	N I	1215.668	H I
1078.708	N IV	1215.674	H I
1083.990	N II	1225.192	N IV
1084.582	N II	1225.719	N IV
1084.908	H ₂ II	1228.790	N I
1084.975	H ₂ II	1230.511	C IV
1085.701	N II	1238.821	N V
1095.940	N I	1243.1796	N I

Wavelength (Å)	Identification	Wavelength (Å)	Identification
1243.3066	N I	1492.6254	N I
1247.383	C III	1494.6751	N I
1256.52	C III	1531.85	C III
1260.613	C I	1548.195	C IV
1260.736	C I	1550.768	C IV
1260.927	C I	1560.6832	C I
1260.996	C I	1561.3407	C I
1261.122	C I	1561.4382	C I
1261.426	C I	1640.474	H• II
1261.552	C I	1657.0078	C I
1270.280	N IV	1699.32	N III
1275.038	N II	1718.551	N IV
1276.201	N II	1740.310	N II
1276.800	N II	1742.7306	N I
1277.550	C II	1743.197	N II
1284.218	N IV	1745.2482	N I
1288.3	C I	1784.85	O III
1289.9	C I	1923.49	O III
1304.8575	O I		
1306.0286	O I		
1310.5401	N I		
1310.9429	N I		
1311.363	C I		
1318.9981	N I		
1319.6760	N I		
1324.40	N III		
1334.5323	C II		
1335.6627	C II		
1335.7077	C II		
1338.603	O IV		
1343.338	N II		
1345.076	N II		
1345.313	N II		
1345.69	N III		
1346.27	N III		
1355.8887	N I		
1357.134	C I		
1359.275	C I		
1371.287	O V		
1379.884	Ar II		
1382.228	Ar II		
1387.31	N III		
1393.755	Si IV ?		
1411.9318	N I		
1411.9494	N I		
1426.45	C III		
1438.37	N IV		
1463.336	C I		



NITROGEN-HELIUM SPECTRUM

FIG. 12

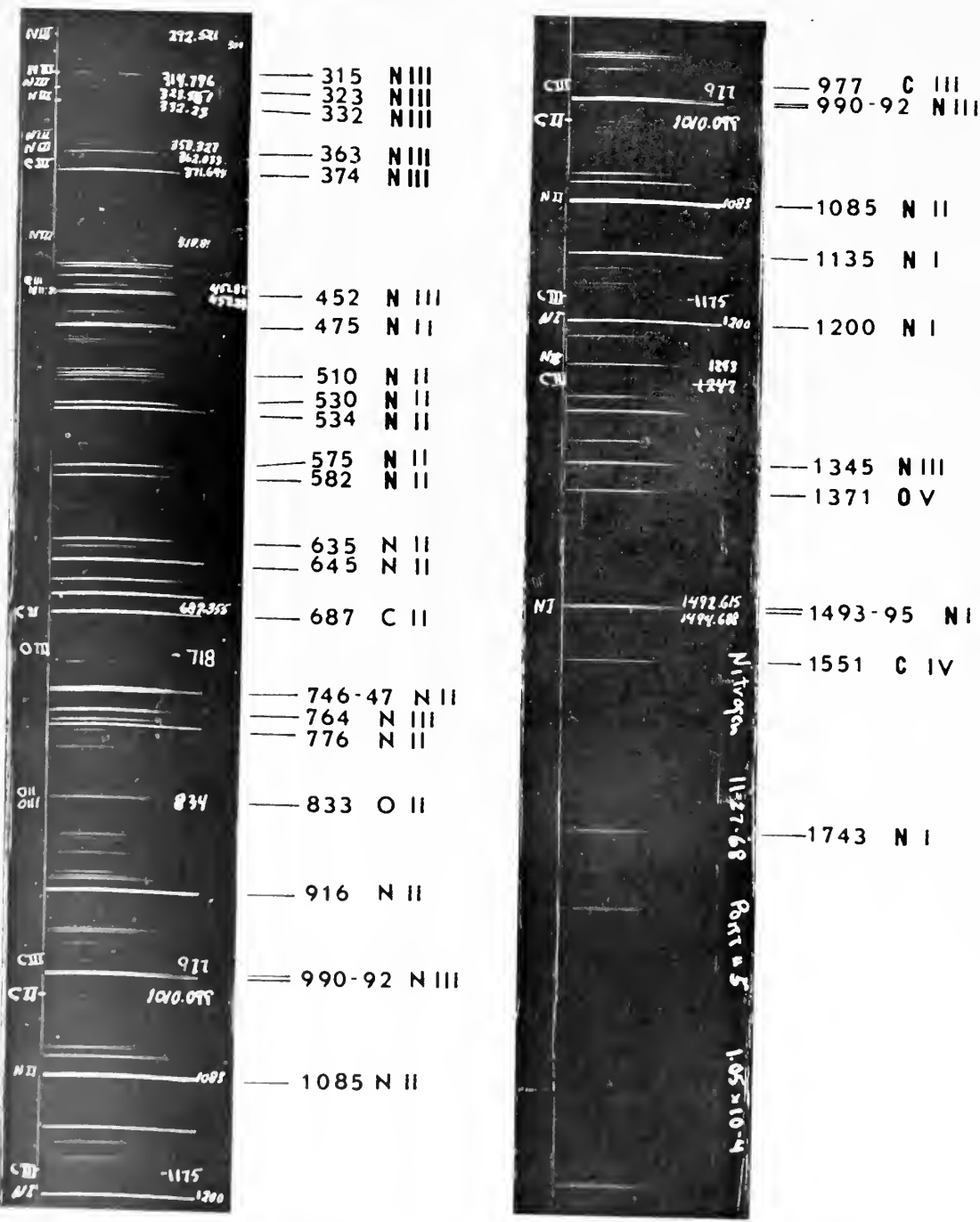


FIG. 13
NITROGEN SPECTRUM

APPENDIX E - GROTRIAN DIAGRAMS

QUARTETS

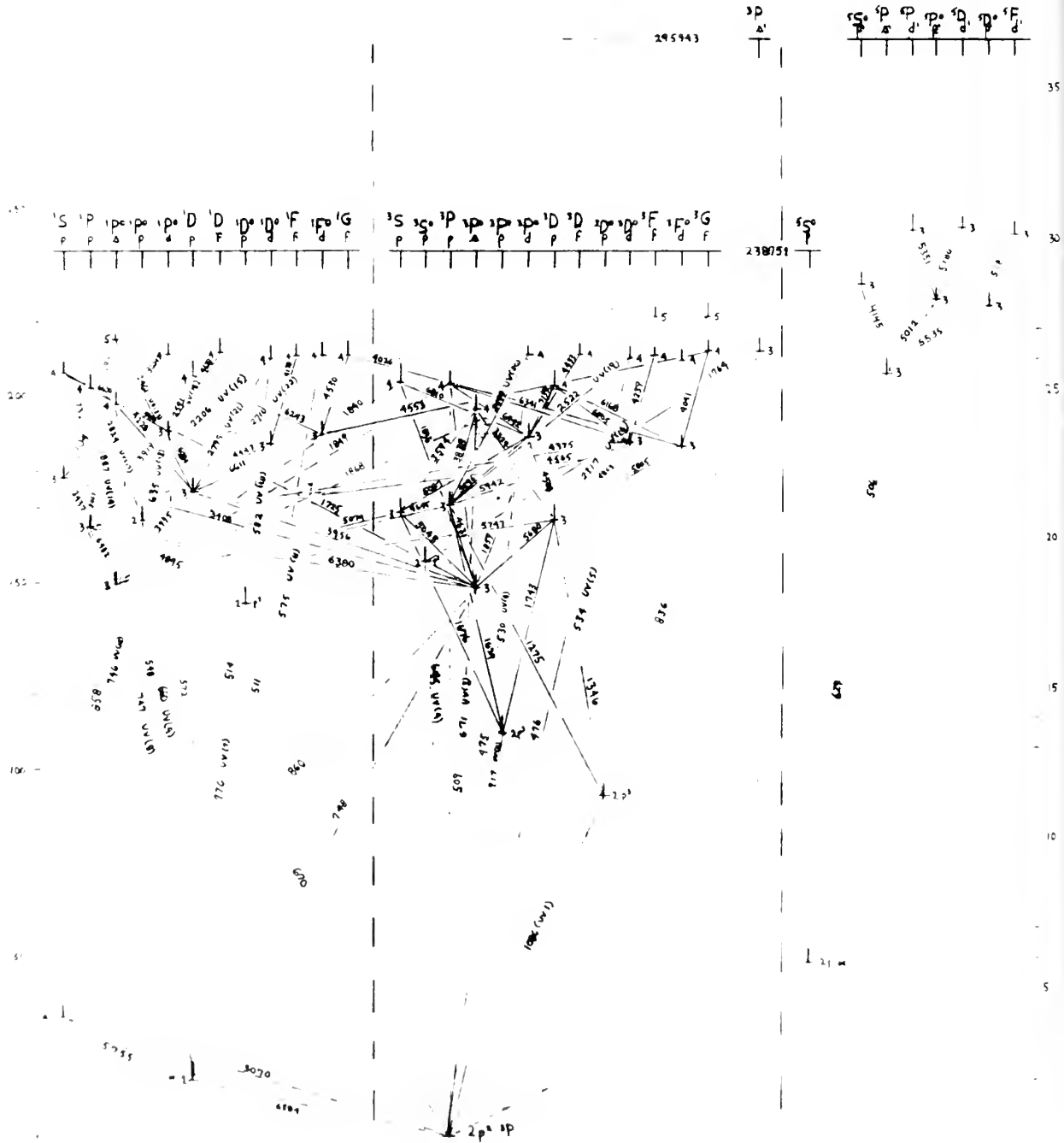
 $1\Delta^2 \ 2\Delta^2 \ 2p^1$

N II

SINGLETs

TRIPLETs

QUINTETs

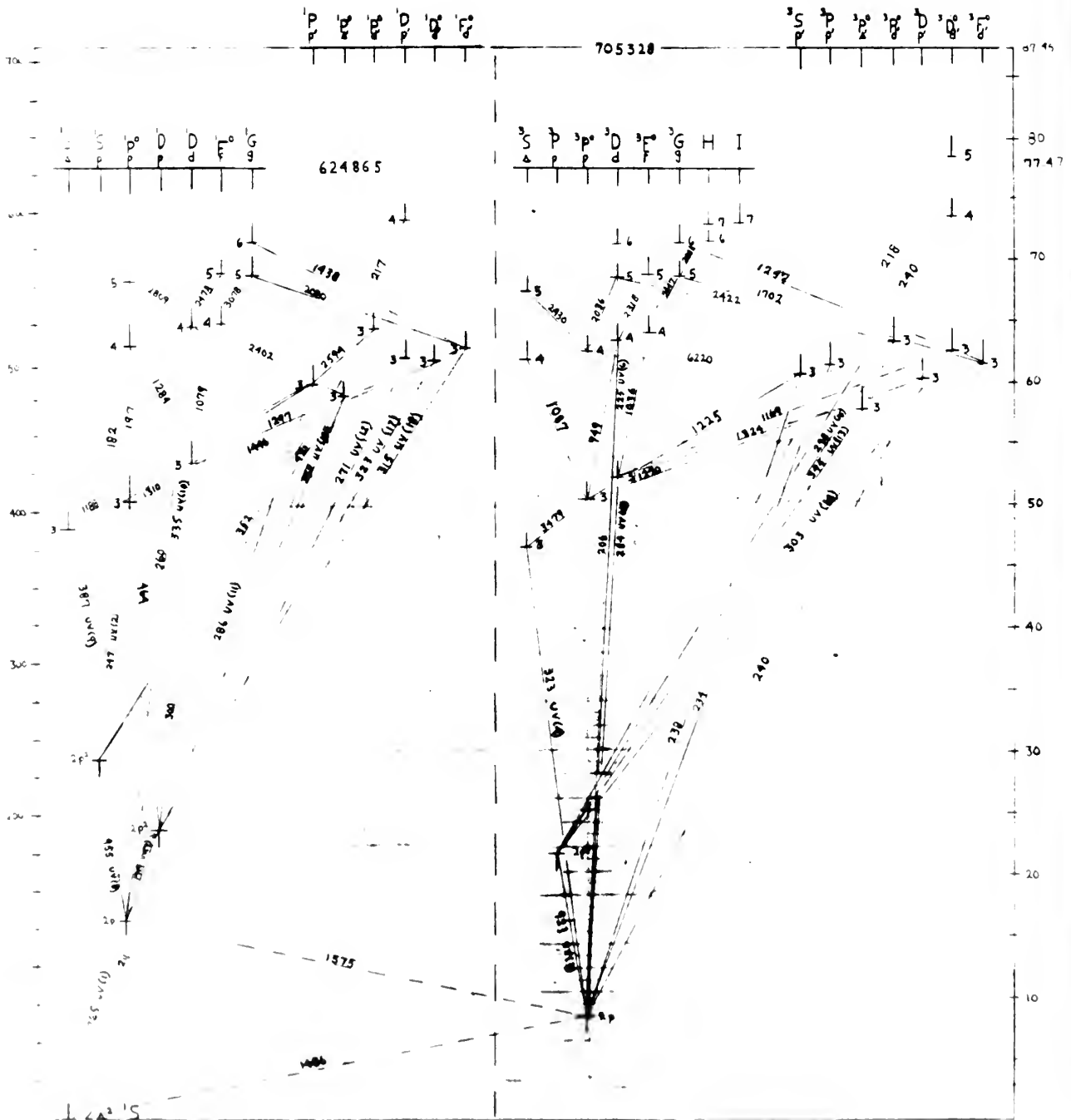


$1s^2 2s^2 2p^2$

NIV

SINGLET S

TRIPLETS


$$1 \Delta^2 \quad 2 \Delta^2$$

71

```

IF 4.1,2X,'VOLTS',//)
202 FORMAT (15X,'MAXIMUM ALLOWABLE INTENSITY RATIO = ',F6.1//15X,
1'MINIMUM ALLOWABLE INTENSITY RATIO = ',F5.2)
205 FORMAT (///25X,'E- TEMPERATURE = ',F7.4,2X,'+/-',2X,F6.4,
12X,'ELECTRON VOLTS',2X,'LTE MODEL',)
206 FORMAT (///25X,'E- TEMPERATURE = ',F7.4,2X,'+/-',2X,F6.4,
12X,'ELECTRON VOLTS',2X,'CORONA MODEL',)
211 FORMAT (///35X,'TEMPERATURE RANGE: ',2X,F7.4,2X,'TO',2X,F7.4)
212 FORMAT (///35X,'PERCENT ERROR = ',2X,F7.2,2X,'PERCENT',)
GAMMA = 1.6
20 READ (5,1) J,JJ
21 IF (J) 100,100,21
21 DO 80 I=1,J
C THE ABOVE DO LOOP CHECKS TO SEE IF ALL DATA HAS BEEN ENTERED
80 READ (5,2) EXCIPO(I),JUPPER(I),JLOW(I),F(I),WL(I),RELINT(I)
C THE ABOVE INSTRUCTION WILL READ DATA ON A SERIES OF "JJ" SPECTRAL
C LINES. WHEN INSERTING THE DATA, ASSURE THAT THE EXCITATION
C POTENTIALS ARE IN INCREASING ORDER.
C IF DENSIOMETRIC DATA IS ENTERED PARAMETER JJ ON THE CONTROL CARD
C MUST BE SET TO A POSITIVE NUMBER.
IF (JJ) 82,82,81
81 WRITE (6,1)
82 GO TO 83
82 WRITE (6,3)
83 DO 22 I=1,J
22 GLOW(I)=(2.0*JLOW(I))+1.0
WRITE (6,4) I,WL(I),EXCIPO(I),JUPPER(I),JLOW(I),F(I),RELINT(I),
1GLOW(I)
RATMAX=4.0
RATMIN=0.25
N=0
WRITE (6,5)
JK=J-1
DO 26 I=1,JK
K=I+1
RELSET=RELINT(I)
WRITE (6,6) WL(I)
DO 66 M=K,J
N=N+1
CRIT=EXCIPO(M)-EXCIPO(I)
IF (CRIT.LT.VE) GO TO 70
C THE ABOVE INSTRUCTION CHECKS TO SEE IF THE DIFFERENCE IN EXCITATION
C POTENTIAL IS GREATER THAN 4.0. THE DIFFERENCE
C MUST BE SEVERAL EV FOR VALID RESULTS.
WAVE=ABS(WL(I)-WL(M))
IF (WAVE.GT.VWL) GO TO 71
C CHECK TO SEE IF THE WAVELENGTH DIFFERENCE IS LESS THAN 500
C ANGSTROMS. THIS ENSURES SAMPLING A SPECTRAL REGION OF

```

```

C
RELATIVELY EQUAL RESPONSE.
IF (JJ) 63,63,62
Y = (RELSET - RELINT(M))/GAMMA
62  RATIO = 10**Y
GO TO 64
63  RATIO = RELSET/RELINT(M)
IF (RATIO.GT.RATMAX) GO TO 72
IF (RATIO.LT.RATMIN) GO TO 73
64  PART = RATIO*(GLOW(M)/GLOW(I))*(F(M)/F(I))*((WL(I)/WL(M))**3)
TEMP(N) = CRIT/ALOG(PART)
TMP(N) = EXCIPO(I)**3/EXCIPO(M)**3)
WRITE(6,7) WL(M), TEMP(N), TMP(N), RATIO
GO TO 66
70  WRITE(6,8) WL(M),CRIT
GO TO 65
71  WRITE(6,87) WL(M), WAVE
GO TO 65
72  WRITE(6,88) WL(M), RATIO
GO TO 65
73  WRITE(6,89) WL(M), RATIO
65  TEMP(N) = 0.0
66  CONTINUE
26  CONTINUE
WRITE(6,200) VWL
WRITE(6,201) VE
WRITE(6,202) RATMAX,RATMIN
K = 0
SUM=0.0
SSUM = 0.0
ASSUM=0.0
DO 27 I=1,N
IF (TEMP(I).EQ.0.0) GO TO 27
K = K + 1
SUM = SUM + TEMP(I)
ASSUM = ASSUM + TMP(I)
SSUM = SSUM + TEMP(I)*TEMP(I)
ASSUM = ASSUM + TMP(I)*TMP(I)
27  CONTINUE
IF (K.LE.1) GO TO 20
Z = K
AVE=SUM/Z
CAVE = ASSUM/Z
SIGM = SQRT((SSUM - (Z*AVE**2))/Z)
CSIGM = SQRT((ASSUM - (Z*CAVE**2))/Z)
SIGB=SIGM/SQRT(Z)
CSIGB = CSIGM/SQRT(Z)
WRITE(6,205) AVE,SIGB

```

```

CAVE=AVE+SIGB
QAVE=AVE-SIGB
WRITE(6,211) PAVE,QAVE
PERR=SIGB*100.0/AVE
WRITE(6,212) PERR,CSIGB
PAVE=CAVE+CSIGB
QAVE=CAVE-CSIGB
WRITE(6,211) PAVE,QAVE
PERR=CSIGB*100.0/CAVE
WRITE(6,212) PERR
GO TO 20
100 STOP
END

```

21.06	0.0	.106	+4621.405E-10	139.75
21.061	1.0	.0798	+4613.887E-10	95.29
21.062	1.0	.320	+4607.167E-10	134.65
21.064	1.0	.0796	+4643.106E-10	206.40
21.07	2.0	.133	+4601.490E-10	147.28
28.36	1.0	.118	+4124.100E-10	34.59
28.361	2.0	.118	+4133.654E-10	54.51
28.362	2.0	.118	+4145.759E-10	62.82
-100	3.0			

SAMPLE PHOTOMETRIC DATA

WAVELENGTH- (Å)	SAMPLE ELECTRON TEMPERATURE OUTPUT	ELECTRON TEMPERATURES, LT _E (eV)	C _{CHCNA} (eV)	INTENSITY RATIO
THE FOLLOWING LINES ARE BASED ON THE WAVELENGTH OF 4621.405E-10				
4613.887E-10	REJECTED: EXCIPC DIFFERENCE TOO SMALL			0.001
4607.166E-10	REJECTED: EXCIPC DIFFERENCE TOO SMALL			0.002
4643.106E-10	REJECTED: EXCIPC DIFFERENCE TOO SMALL			0.004
4601.490E-10	REJECTED: EXCIPC DIFFERENCE TOO SMALL			0.010
4124.100E-10	REJECTED: INTENSITY RATIO TOO LARGE	3.8545	7.2920	2.5637
4133.654E-10		3.5106	6.1520	2.2246
4145.759E-10				
THE FOLLOWING LINES ARE BASED ON THE WAVELENGTH OF 4613.887E-10				
4607.166E-10	REJECTED: EXCIPC DIFFERENCE TOO SMALL			0.001
4643.106E-10	REJECTED: EXCIPC DIFFERENCE TOO SMALL			0.003
4601.490E-10	REJECTED: EXCIPC DIFFERENCE TOO SMALL			0.009
4124.100E-10		4.1920	8.6021	2.7549
4133.654E-10		4.0776	8.1340	1.7481
4145.759E-10		3.6947	6.7404	1.5169
THE FOLLOWING LINES ARE BASED ON THE WAVELENGTH OF 4607.166E-10				
4643.106E-10	REJECTED: EXCIPC DIFFERENCE TOO SMALL			0.002
4601.490E-10	REJECTED: EXCIPC DIFFERENCE TOO SMALL			0.008
4124.100E-10		4.0717	8.1102	3.8927
4133.654E-10		3.9637	7.6928	2.4702
4145.759E-10		3.6009	6.4345	2.1434
THE FOLLOWING LINES ARE BASED ON THE WAVELENGTH OF 4643.106E-10				
4601.490E-10	REJECTED: EXCIPC DIFFERENCE TOO SMALL			0.006
4124.100E-10	REJECTED: WAVELENGTH DIFFERENCE TOO LARGE			519.006E-10
4133.654E-10	REJECTED: WAVELENGTH DIFFERENCE TOO LARGE			509.452E-10
4145.759E-10		3.2298	5.3392	3.2856
THE FOLLOWING LINES ARE BASED ON THE WAVELENGTH OF 4601.490E-10				
4124.100E-10	REJECTED: INTENSITY RATIO TOO LARGE			4.258
4133.654E-10				
4145.759E-10				
THE FOLLOWING LINES ARE BASED ON THE WAVELENGTH OF 4124.100E-10				
4133.654E-10	REJECTED: EXCIPC DIFFERENCE TOO SMALL			0.001
4145.759E-10	REJECTED: EXCIPC DIFFERENCE TOO SMALL	4.2718	8.9431	2.7010
THE FOLLOWING LINES ARE BASED ON THE WAVELENGTH OF 4133.654E-10				
4145.759E-10	REJECTED: EXCIPC DIFFERENCE TOO SMALL	3.8530	7.2849	2.3445

MAXIMUM WAVELENGTH DIFFERENCE = 500.0F-10 METERS

MINIMUM EXCITATION POTENTIAL DIFFERENCE = 4.0 VOLTS

MAXIMUM ALLOWABLE INTENSITY RATIO = 4.0

MINIMUM ALLOWABLE INTENSITY RATIO = 0.25

E- TEMPERATURE = 3.8473 +/- 0.0907 ELECTRON VOLTS LTE MODEL

TEMPERATURE RANGE: 3.9380 TO 3.7566

PERCENT ERROR = 2.36 PERCENT

E- TEMPERATURE = 7.3385 +/- 0.3164 ELECTRON VOLTS CORONA MODEL

TEMPERATURE RANGE: 7.6550 TO 7.0221

PERCENT ERROR = 4.31 PERCENT

RELATIVE INTENSITY COMPUTER PROGRAM

```

C THIS PROGRAM IS DESIGNED TO CALCULATE RELATIVE
C INTENSITIES BASED ON INPUT WAVELENGTH AND
C EXCITATION POTENTIALS. RELATIVE INTENSITIES
C ARE CALCULATED BY SELECTING THE TRANSITION
C WITH THE LARGEST EXCITATION POTENTIAL AS
C ARBITRARILY EQUAL TO AN INTENSITY OF 100. FOR
C RELATIVE INTENSITIES ARE THEN CALCULATED FOR
C BOTH THE LTE AND CORONA PLASMA RADIATION
C MODEL MIX RESULTS.
C DIMENSION GLOW(50), EXCIPO(50), LOCINT(50), WL(50), JLOW(50),
C 1 JUPPER(50), CORINT(50), MIX(6)
C REAL LOCINT, MIX, JUPPER, JLOW
C 1 FORMAT(I5)
C 2 FORMAT(4F10.0, E13.0)
C 3 FORMAT(11, 5X, 'NO.', 4X, 'WAVELENGTH', 7X, 'EXCITATION POTENTIAL',
C 11X, 'J', 17X, 'J', 11X, 'ABSORPTION', 2X, 'LTE RELATIVE', 3X, '2J+1', /14X,
C 21 (METERS), 15X, '(VOLTS)', 11X, '(UPPER LEVEL)', 5X, '(LOWER LEVEL)',
C 36X, 'STRENGTH', 5X, 'INTENSITY', 4X, '(LCW)', /)
C 4 FORMAT(1, 5X, 14, 2X, 3PE13.3, 12X, OPF7.3, 17X, F3.1, 15X, F3.1, 11X, F8.5,
C 16X, F7.2, 5X, F4.1)
C 5 FORMAT(1, 30X, 'INTENSITIES FROM MODEL MIX', //, ' WAVELENGTH
C 1 LTE 80%LTE 60%LTE 40%LTE 20%LTE
C 6 FORMAT(3PE13.3, OPF10.3, 5F10.3)
C CHANGED FOR UV SPECTRA
C VE=4.0
C 20 READ(5,1) J
C IF(J) 100,100,21
C 21 DO 80 I=1,J
C THE ABOVE DO LOOP CHECKS TO SEE IF ALL DATA HAS BEEN ENTERED
C READ(5,2) EXCIPO(I), JUPPER(I), JLOW(I), F(I), WL(I)
C CONTINUE
C THE ABOVE INSTRUCTION WILL READ DATA ON A SERIES OF "J" SPECTRAL
C LINES.
C DO 50 I = 1, J
C GLOW(I) = (2.0*JLOW(I))+1.0
C DO 60 ITEMP = 4, 8
C ITEMP = ITEMP
C LOCINT(J)=100.0
C I = 2
C CRIT = EXCIPO(J) - EXCIPO(1)
C CONST = 100.0*((GLOW(1)*F(1))/(GLOW(J)*F(J)))*
C 1((WL(J)/WL(1))**3)

```

```

LOCINT(1) = CONST*EXP(CRIT/ETEMP)
CORINT(1) = LOCINT(1)*(EXCIPO(J)**3/EXCIPO(1)**3)
CORINT(J) = 100.0*(EXCIPO(1)**3/EXCIPO(J)**3)
52 CRIT = EXCIPO(J) - EXCIPO(1)
IF (ABS(CRIT).GT.VE) GO TO 54
CRIT = EXCIPO(1) - EXCIPO(J)
CONST=((GLOW(I)*F(I))/(GLOW(1)*F(1)))*
1((WL(1)/WL(I))**3)
LOCINT(I)=CONST*LOCINT(1)*EXP(CRIT/ETEMP)
CORINT(I) = LOCINT(I)*(EXCIPO(1)**3/EXCIPO(I)**3)
53 I = I+1
IF (I.GE.J) GO TO 55
GO TO 52
54 CONST=((GLOW(I)*F(I))/(GLOW(J)*F(J)))*
1((WL(J)/WL(I))**3)
LOCINT(I)=CONST*LOCINT(J)*EXP(CRIT/ETEMP)
CORINT(I) = LOCINT(I)*(EXCIPO(J)**3/EXCIPO(I)**3)
GO TO 53
55 WRITE (6,3)
DO 56 I = 1,J
56 WRITE (6,4) I,WL(I),EXCIPO(I),JUPPER(I),JLOW(I),F(I),LOCINT(I),
1GLOW(I)
WRITE (6,5)
DO 58 IL = 1,J
58 IL = LOCINT(IL) + .2*CORINT(IL)
MIX(1) = .8*LOCINT(IL) + .4*CORINT(IL)
MIX(2) = .6*LOCINT(IL) + .6*CORINT(IL)
MIX(4) = .4*LOCINT(IL) + .8*CORINT(IL)
MIX(5) = .2*LOCINT(IL) + .8*CORINT(IL)
MIX(6) = CORINT(IL)
WRITE(6,6) WL(IL),MIX(IK),IK=1,6)
58 CONTINUE
60 CONTINUE
100 GO TO 20
STOP
END

```

	SAMPLE DATA					
18.38	0.0	0.01050	+671.8E-10			
18.39	1.0	0.00785	+671.6E-10			
18.39	2.0	0.00785	+672.0E-10			
18.39	0.0	0.03130	+671.4E-10			
18.40	2.0	0.0233	+671.4E-10			
18.40	1.0	0.01290	+671.0E-10			

COMPUTER PROGRAM GLOSSARY

AVE = AVERAGE ELECTRON TEMPERATURE (EV)
 CORINT = CORONA MODEL INTENSITY
 CRIT = EXCITATION ENERGY DIFFERENCE
 EXCIPO = EXCITATION ENERGY OF SPECTRAL LINE
 F = ABSORPTION OSCILLATOR STRENGTH
 GAMMA = SLOPE OF LOG RELATIVE DENSITY VS LOG EXPOSURE
 GLOW = STATISTICAL WEIGHT OF LOWER STATE OF SPECTRAL LINE
 ITEMP = ELECTRON TEMPERATURE SET FOR RELATIVE INTENSITY PROGRAM
 JLOW = SPIN-ORBITAL ANGULAR MOMENTUM QUANTUM NUMBER OF LOWER STATE
 JUPPER = SPIN-ORBITAL ANGULAR MOMENTUM QUANTUM NUMBER OF UPPER STATE
 LOCINT = LOCAL THERMAL EQUILIBRIUM RELATIVE INTENSITY
 LTE = LOCAL THERMAL EQUILIBRIUM
 MIX = LINEAR COMBINATION OF LTE AND CORONA MODEL RELATIVE INTENSITIES
 PAVE = AVERAGE ELECTRON TEMPERATURE + STANDARD DEVIATION OF THE MEAN
 PERR = (STANDARD DEVIATION OF THE MEAN / AVERAGE ELECTRON TEMPERATURE) * 100.0
 QAVE = AVERAGE ELECTRON TEMPERATURE - STANDARD DEVIATION OF THE MEAN
 RATIO = RELATIVE INTENSITY RATIO
 RATMAX = MAXIMUM INTENSITY RATIO
 RATMIN = MINIMUM INTENSITY RATIO
 RELINT = RELATIVE INTENSITY (OR DENSITY) OF SPECTRAL LINE
 RELSET = BASE RELATIVE INTENSITY FOR ELECTRON TEMPERATURE CALCULATIONS
 SIGB = STANDARD DEVIATION OF THE MEAN
 SIGM = STANDARD DEVIATION
 TEMP = LTE MODEL ELECTRON TEMPERATURE (EV)
 TMP = CORONA MODEL ELECTRON TEMPERATURE (EV)
 VE = MINIMUM EXCITATION ENERGY DIFFERENCE
 VWL = MAXIMUM WAVELENGTH DIFFERENCE
 WAVE = WAVELENGTH DIFFERENCE
 WL = WAVELENGTH

NOTE: TERMS USED IN COMPUTING AVERAGE VALUES AND DEVIATIONS MAY BE MODIFIED BY PREFIX "C" TO INDICATE CORONA MODEL CALCULATIONS

BIBLIOGRAPHY

1. Andrews, R. C., Shock Production, Langmuir Probe Diagnostics, and Instabilities in a Nitrogen Plasma, Master's Thesis, Naval Postgraduate School, Monterey, California, 1968.
2. Orlicki, G. A., Spectroscopic Diagnostics of a Nitrogen Plasma, Master's Thesis, Naval Postgraduate School, Monterey, California, 1968.
3. Kaufman, L. E., Investigations in the Vacuum Ultraviolet Using a Grazing Incidence Spectrograph, Master's Thesis, Naval Postgraduate School, Monterey, California, 1967.
4. Samson, J. A. R., Techniques of Vacuum Ultraviolet Spectroscopy, p. 34-40, Wiley, 1967.
5. Beutler, H. G., "The Theory of the Concave Grating," J. Optical Society of America, v. 35, p. 311ff, May, 1945.
6. Samson, J. A. R., op cit, p. 11-14.
7. Orlicki, G. A., op cit.
8. Rose, D. J., and Clark, M. Jr., Plasmas and Controlled Fusion, p. 165-172, MIT Press and Wiley, 1961.
9. Huddleston, R. H., and Leonard, S. L., (ed), Plasma Diagnostic Techniques, R. W. P. McWhirter, "Spectral Intensities," p. 201-261, Academic Press, 1965.
10. Griem, H. R., Plasma Spectroscopy, p. 129-167, 267-278, 425-431, McGraw-Hill, 1964.
11. Robinson, D. and Lenn, P. D., "Plasma Diagnostics by Spectroscopic Methods," Applied Optics, v. 6, No. 6, p. 983-1000, June 1967.
12. Wiese, W. L., Smith, M. W., and Glennon, B. M., Atomic Transition Probabilities, v. 1, Hydrogen through Neon, NSRDS-NBS4, Government Printing Office, May 20, 1966.
13. Kelly, R. L., A Grazing Incidence Vacuum Spectrograph of Simple Design, Stanford Research Institute, December 31, 1959.
14. Kaufman, L. E., op cit.
15. Harrison, G. R., Lord, R. S., and Loofbourow, J. R., Practical Spectroscopy, p. 356, Prentice-Hall, 1948.
16. Eastman Kodak Company, Kodak Plates and Films for Science and Industry.

17. Moore, C. E., Atomic Energy Levels, Vol. I, p. 32-42, NBS 467, Government Printing Office, June 15, 1949.
18. Moore, C. E., An Ultraviolet Multiplet Table, NBS 488, Section 4, Government Printing Office, April 6, 1962.
19. Kelly, R. L., Atomic Emission Lines Below 2000 Angstroms, Hydrogen through Argon, Naval Research Laboratory 6648, February, 1968.
20. Samson, J. A. R., op cit, p. 43-83.
21. Keller, L. R., Ultraviolet Radiation, 2d ed., Wiley, 1965.

INITIAL DISTRIBUTION LIST

	No. Copies
1. Defense Documentation Center Cameron Station Alexandria, Virginia 22314	20
2. Library, Code 0212 Naval Postgraduate School Monterey, California 93940	2
3. Defense Atomic Support Agency Department of Defense Washington, D. C. 20305	1
4. Assoc. Professor A. W. Cooper, 61 Cr Department of Physics Naval Postgraduate School Monterey, California 93940	4
5. LCDR James C. Beam, USN P. O. Box 610 Fort Myers, Florida 33902	2
6. Professor Norman L. Oleson Department of Physics University of South Florida Tampa, Florida 33620	1

DOCUMENT CONTROL DATA - R & D

Security classification of title, body of abstract and indexing annotation must be entered when the overall report is classified

1. ORIGINATING ACTIVITY (Corporate author) Naval Postgraduate School Monterey, California 93940		2a. REPORT SECURITY CLASSIFICATION Unclassified	
		2b. GROUP	
3. REPORT TITLE Investigations in the Vacuum Ultraviolet of a Steady State Nitrogen Plasma			
4. DESCRIPTIVE NOTES (Type of report and, inclusive dates) Master's Thesis, June 1969			
5. AUTHOR(S) (First name, middle initial, last name) James C. Beam			
6. REPORT DATE June 1969	7a. TOTAL NO. OF PAGES 84	7b. NO. OF REFS 21	
8a. CONTRACT OR GRANT NO.	9a. ORIGINATOR'S REPORT NUMBER(S)		
b. PROJECT NO.			
c.	9b. OTHER REPORT NO(S) (Any other numbers that may be assigned this report)		
d.			
10. DISTRIBUTION STATEMENT Distribution of this document is unlimited.			
11. SUPPLEMENTARY NOTES		12. SPONSORING MILITARY ACTIVITY Naval Postgraduate School Monterey, California 93940	
13. ABSTRACT In preparation for studies of shock waves in a collisionless plasma, a grazing incidence vacuum spectrograph has been used to study the vacuum ultraviolet spectra of a nitrogen plasma. The spectra are formed by a concave grating with a 1-meter radius of curvature and recorded on Kodak SWR (Shortwave-Radiation) Film. Analysis of the spectra was by comparison with helium and argon spectra, with intensity information from densitometric measurement using a Leeds and Northrup recording densitometer. Relative intensity determination provides an electron temperature evaluation technique. Details on the modification of the Naval Postgraduate School plasma facility to accommodate a theta-pinch shock generation experiment are presented. Revised operating procedures for the new system configuration are included in the appendix. A total of 735 lines was observed in the range 300-2000 angstroms. Relative intensity measurements indicated electron temperatures in the range 7.3 to 19.7 electron volts. Predicted relative intensities using a variable combination of the Local Thermal Equilibrium and Corona plasma models showed good sensitivity to temperature, but little difference between models.			

Unclassified

Security Classification

14

KEY WORDS

LINK A

LINK B

LINK C

ROLE

WT

ROLE

WT

ROLE

WT

plasma spectroscopy

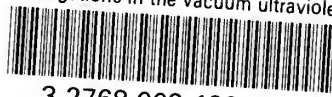
ultraviolet

nitrogen



thesB287

Investigations in the vacuum ultraviolet



3 2768 002 12882 9
DUDLEY KNOX LIBRARY